



JOINT MEETING

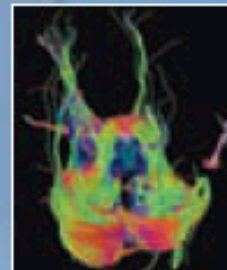
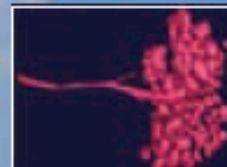
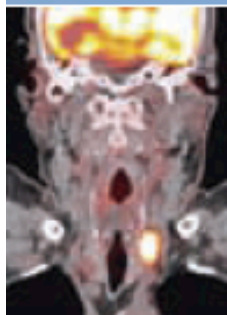
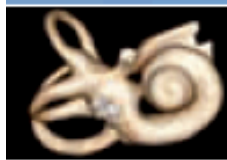
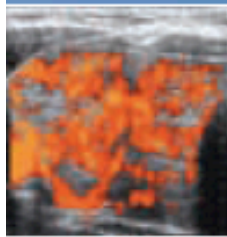
**EUROPEAN SOCIETY
OF HEAD AND
NECK RADIOLOGY**

21st Annual Meeting
and Refresher Course
www.eshnr2008.org

GENEVA, SWITZERLAND
6-8 November 2008

**SWISS SOCIETY OF
OTORHINOLARYNGOLOGY
– HEAD & NECK SURGERY**

www.orl-hno.ch





21st Annual Meeting and Postgraduate Course of the
European Society of Head and Neck Radiology (ESHNR)

and

94th Postgraduate Course of the Swiss Society of
Otorhinolaryngology Head and Neck Surgery (SSORL)

**Abstract Book
of
Oral Presentations and Scientific Posters**

CICG, November 6 – 8, 2008

Table of Contents

P. Alves, A. Borges Buccal space revisited ? A guided tour through the buccal space Poster Nr 1	9
M. Anooshiravani, R. Kohler, B. Pittet, B. Rillet, M. Becker Inflammatory myofibroblastic tumor of the nasal cavity in a 6 year old child Poster Nr 2	10
J. Aw, M.E. Williams, V.Beric Comparison of conventional and MR sialography with clinical correlation in benign salivary gland disease Poster Nr 3	11
J. Aw, J. Searle, G. McGann, I. Hagan, E. Brown, I. Lyburn Physiological and benign causes of F-18 fluorodeoxyglucose (FDG) uptake within the head and neck on PET/CT imaging Poster Nr 4	12
D.J. Bell, T. Beale Beware: the salivary gland pseudomass Poster Nr 5	13
D.J. Bell, S.E.J. Connor The CT appearances of normal and abnormal craniofacial topographical anatomy Poster Nr 6	14
D.J. Bell, E.K. Woo Multidetector CT in the investigation of vocal cord palsy Poster Nr 7	15
D.J. Bell, S.E.J. Connor Rhinolithiasis Poster Nr 8	16
B.I. Berg-Boerner, C. Kunz, K. Schwenzer-Zimmerer, E.W. Radü, C. Kober, K. Scheffler, C. Buitrago-Téllez, A. Palmowski-Wolfe Dynamic ocular MRI- comparison of clinical testing and imaging Poster Nr 9	17
S. Bisdas, M.G. Mack, G. Glavina, K. Surlan-Popovic, T.J. Vogl, Z. Rumboldt Outcome prediction after surgery and chemoradiation of squamous cell carcinoma in the oral cavity, oropharynx and hypopharynx : perfusion CT parameters versus tumor volume Oral presentation	18
S. Bisdas, Z. Rumboldt, K. Spicer, T.J. Vogl, M.G. Mack Tissue perfusion and glucose metabolism coupling in head and neck squamous cell carcinomas using combined PET/CT imaging Oral presentation	19
S. Bisdas, Z. Rumboldt, M. Baghi, J. Wagenblast, K. Surlan-Popovic, T.J. Vogl, M.G. Mack Prediction of tumor response and recurrence in advanced squamous cell carcinoma of the oropharynx: The use of pre-treatment dynamic contrast-enhanced CT microcirculatory parameters versus tumor volume Poster Nr 10	20

M. Bongiovanni, P. Dulguerov, A. Lobrinus, K. Burkhardt, M. Gremaud, M. Becker The utility of whole organ macrosection technique in the management of head and neck tumors and its correlation to preoperative imaging Poster Nr 11	21
K.M. Chew, J.P.N. Goh The spectrum of imaging findings of ingested gastrointestinal foreign bodies Poster Nr 12	22
S.E.J. Connor, D.J. Bell CT and MRI cochlear diameter measurements may predict electrode length to 360 degrees insertion depth angle Oral presentation	23
R.B.J. de Bondt, M.C. Hoerberigs, P.J. Nelemans, W. Deserno, J.W. Casselman, J. Verwoerd, B. Kremer and R.G.H. Beets-Tan Diagnostic accuracy of DWI ?MRI for discrimination of cervical metastatic lymph nodes in head and neck squamous cell carcinoma Oral presentation	24
A. Delantoni An unusual iatrogenic unilateral fracture of the coronoid process of the mandible that was not diagnosed for 12 years by both radiologists and dentists Poster Nr 13	25
A.H El Beltagi, K. El Sebeih, N. El Shemari, L. Al Rabiaa Aural lesions imaging, the tip of the iceberg Poster Nr 14	26
G. Gavridakis, E. Astropekaki, E. Manolakakis, S. Stagkouraki, G. Liodakis, K. Psaras, N. Syrmos, L. Triantafyllou Agensis of the sphenoid sinus Poster Nr 15	27
A. Germano, I. Cravo, T. Palma, E. Serrão, G. Alves Pharyngeal wall bulging. What we found behind it Poster Nr 16	28
D. Gibson, A. Whyte, S. Karamfiles, M. Atlas Use of high-resolution DRIVE sequences to establish the variability in the orientation of the osseous spiral lamina along the basal turn of the cochlear in twenty normal hearing individuals ? A potential role prior to cochlea surgery Oral presentation	29
Y. Gupta, N. Stephens, T. Beale Diagnostic adequacy of ultrasound guided fine needle aspiration cytology in neck lump investigation: a comparative audit of three reporting setups Oral presentation	30
H. Haba Radiologic-pathologic correlations in complicated cases of head and neck tuberculosis Poster Nr 17	31
C.R. Habermann, C. Arndt, J. Graessner, F. Reitmeier, M. Jaehne, G. Adam Diffusion-weighted echo-planar MRI: still a valuable tool for differentiating primary parotid gland tumors in a large patient collective ? Oral presentation	32

C.R. Habermann, T. Ries, C. Arndt, M. Regier, J. Graessner, M.C. Cramer, F. Reitmeier, M. Jaehne, G. Adam Value of apparent diffusion coefficient calculation before and after gustatory stimulation in the diagnosis of acute or chronic parotitis Oral presentation	33
C.R. Habermann, C. Arndt, J. Graessner, F. Reitmeier, M. Jaehne, G. Adam Differentiation of primary parotid gland tumors: does the combination of diffusion weighted echo-planar MRI and magnetization transfer imaging offers diagnostic improvement ? Poster Nr 18	34
E. Kamel Dynamic contrast-enhanced MR imaging: a reliable diagnostic tool for recurrent head and neck tumors Oral presentation	35
J.H. Kim, D.S. Kim, K.H. Chang Ultrasonographic features of follicular variant papillary thyroid carcinoma: mimicker of a benign thyroid nodule Oral presentation	36
.H. Kim, M.H. Yu, K.H. Chang To evaluate the MR features in patients with nasopharyngeal tuberculosis Poster Nr 19	37
S.J. Kim Preoperative thyroid cancer staging: what the radiologist should know Poster Nr 20	38
Y. Kim, B. Kim, H. Song CT characteristics of benign and malignant lesions of the jawbones Poster Nr 21	39
C. Kober, I.B. Berg, S. Berg, R. Sader, H.F. Zeilhofer A systematic approach of 3D-visualization of the ethmoid air cells and craniofacial sinuses based on clinical CT Poster Nr 22	40
R. Kohler, M. Viallon, X. Montet, M. Becker Can diffusion-weighted MR imaging differentiate benign from malignant tumors in the head and neck ? Oral presentation	41
R. Kohler, I. Masouye, M. Becker Contribution of MRI for detection of late complications of facial plastic surgery Poster Nr 23	42
R. Kohler, M.I. Vargas, K.O. Lövblad, J. Delavelle, P.A. Poletti, M. Becker Contribution of the CT and MRI angiography in the diagnosis of traumatic vascular injuries in the head and neck Poster Nr 24	43
S. La'Porte, J.K. Juttla, H. Lloyd-Hughes, D. Remedios Cervical tuberculous adenitis: what are the most reliable ultrasound features ? Oral presentation	44
S. La'Porte, J.K. Juttla, H. Lloyd-Hughes, D. Remedios Neck TB or not TB: the value of ultrasound, cytology and microbiology for diagnosis Oral presentation	45

S.Y. Lee, M.H. Jeon, I.H. Bae, G.S. Han, S.H. Cha, S.G. Kim, K.S. Park Narrow duplicated or triplicated internal auditory canal: CT finding of three cases And review of the literature Poster Nr 25	46
R.K. Lingam, S. Kaneira, M. Qarib Evaluating thyroid nodules: can ultrasound accurately predict and select neoplastic nodules for fine needle aspiration (FNA) cytology Oral presentation	47
A. Lo Casto, F. Ganguzza, P. Collodoro, G. Cavarretta, A. Comparetto, G. La Tona Multidetector CT (MDCT) in the diagnosis of sinonasal osteoma Oral presentation	48
A. Lo Casto, F. Coppolino, F. Ganguzza, S. Salerno, R.T. Bruno, G. La Tona Langerhans cell histiocytosis (LCH) of the jaws. Panoramic radiography, CT and MRI findings Poster Nr 26	49
L. Lopes, D. Coutinho Tongue hemiatrophy: a silent sign for skull base pathology Poster Nr 27	50
K. Masterson, R. Kohler, O. Ratib, C. Steiner, M. Becker PET-CT pitfalls in head and neck pathologies Poster Nr 28	51
K. Masterson, R. Kohler, M.I. Vargas, J. Delavelle, M. Bongiovanni, M. Becker Tumors and tumor-like lesions of the orbit: radiologic-pathologic correlation Poster Nr 29	52
T. Nakasato, M. Hitachi, H. Oikawa, R. Nakamura, S. Ehara, M. Izumisawa Intra-arterial infusion chemotherapy for head and neck SCCs with mandibular invasion Poster Nr 30	53
S.F. Nemeč, P.C. Brugger, C. Czerny, D. Prayer The face predicts the brain: the association of facial malformations and brain anomalies in fetuses with trisomy 13 in fetal MRI Oral presentation	54
T. Palma, I. Cravo, C. Gonçalves, A. Germano, S. Costa, A. Valverde Cranial neuropathies as a manifestation of systemic disease Poster Nr 31	55
S.H. Park, J.Y. Kwak, S.J. Kim, M.J. Kim, E.K. Kin Interobserver agreement at the malignant thyroid nodules with conventional ultrasound (US) and US elastography: prospective study Oral presentation	56
F. Pekiner, K. Orhan, P. Berglund, L.T. Flygare Comparison of low-dose with standard-dose and an optimized FESS-protocol in multidetector CT examinations of paranasal sinuses Poster Nr 32	57
M. Ravanelli, D. Farina, E. Botturi, A. Borghesi, R. Maroldi Image fusion between echo-planar diffusion-weighted (EP-DW) and isotropic 3D VIBE post-Gd in head and neck: a feasibility study. Oral presentation	58

M. Ravanelli, D. Farina, E. Botturi, A. Borghesi, R. Maroldi Optimization of echo-planar diffusion-weighted (EP-DWI) sequences in the head and neck: signal/noise ratio and ghosting artifacts Oral presentation	59
O. Saborowski, F. Santini, M. Fani, K. Mueller, P. Robert, J.M. Froehlich, G. Bongartz MR Imaging of a human nasopharynx tumor on a cellular level using iron oxide nanoparticles of different sizes Poster Nr 33	60
N.S. Serova., A.Y. Vasiliev, A.I. Ushakov, I.N. Gipp Comparable evaluation of radiological methods in dental implantology based on evidential medicine principles Poster Nr 34	61
H.H. Song, Y.J. Kim, B.S. Kim CT and MR evaluation of proptosis Poster Nr 35	62
T. Stavric, N. Sekularac, I. Jovanovic-Stavric Neck phlegmon with fistula-case report Poster Nr 36	63
S.C.A. Steens, B. De Foer, R. Hermans, B.M. Verbist "Diseased mastoid air cell" due to epineurial pseudocyst of the intratemporal facial nerve Poster Nr 37	64
N.J. Stephens, S. Punwani, T. Beale, S. Morley MR imaging of the larynx - the way forward ? Oral presentation	65
N.J. Stephens, S. Brown, E.J. Adam Imaging assessment of lymph nodes Poster Nr 38	66
N.J. Stephens, S. Morley, T. Beale Laryngeal ultrasound Poster Nr 39	67
N.J. Stephens, S. Morley, A. Ahmed, T. Beale Ultrasound of the thyroid: a pictorial review Poster Nr 40	68
N.J. Stephens, A. Ahmed, T. Beale, S. Morley Top ten tips for ultrasound guided FNA in the neck Poster Nr 41	69
D.B. Stobo, G.T.J O'Neill Does upper aerodigestive tract tumour site influence incidence of intrathoracic malignancy at initial staging ? Oral presentation	70
K. Surlan-Popovic, Z. Rumboldt, T.J. Vogl, M.G. Mack, S. Bisdas Squamous cell carcinoma perfusion at multi-detector row CT: reproducibility of tumor and muscle quantitative measurements, inter- and intra-observer agreement Oral presentation	71

K. Surlan-Popovic, Z. Rumboldt, M.V Spampinato, T.J. Vogl, M.G. Mack, S. Blsdas Perfusion CT of the cervical spinal cord: feasibility and reproducibility of the method and interchangeability of the perfusion estimates between two software packages Poster Nr 42	72
N. Syrmos, G. Gavridakis, E. Astropekaki, K. Grigoriou, V. Valadakis, D. Arvanitakis, L. Triantafyllou Evaluation with cranial computed tomography as a prognostic factor for head injuries in children and young adolescents Poster Nr 43	73
N. Syrmos, G. Gavridakis, E. Astropekaki, K. Grigoriou, V. Valadakis, D. Arvanitakis, L. Triantafyllou Traumatic brain injuries in rural areas of Crete Poster Nr 44	74
L. Trevisiol, E. Grendene, A. D'Agostino, G. Bissolotti, G. Corrocher, R. Maroldi, M. Pregarz, P.F. Nocini The accuracy of 3D CBCT in diagnosis and treatment planning of dentofacial deformities Poster Nr 45	75
A. Trojanowska, P. Trojanowski, W Olszanski, J Klatka, A. Drop CT perfusion examination is useless in evaluation of mandibular infiltration by malignant tumor - true or false ? Oral presentation	76
D.W. Tshering, H.C. Thoeny, S. Ross, D. Spendlove, S. Bolliger, M.J. Thali, P. Vock, L. Oesterhelweg, A. Christe MRI findings in the neck of survivors of strangulation Oral presentation	77
D.W. Tshering, S. Simon-Zoula, P. Zbaeren, A. Geretschlaeger, H.C. Thoeny The role of DW-MRI in the differentiation of tumor and posttherapeutic changes after radiotherapy of laryngeal or hypopharyngeal cancers Oral presentation	78
J. Vallo, L. Suominen-Taipale, A. Norblad, S. Huuonen, K. Soikkonen Maxillary sinus findings in relation to dental findings Poster Nr 46	79
C. Vandervelde, S. Connor Diagnostic yield of MRI for audiovestibular dysfunction using contemporary referral criteria: correlation with presenting symptoms and impact on clinical management Oral presentation	80
M.I. Vargas, M. Viallon, R. Kohler, M. Becker, K.O. Lövblad, S. Altrichter, J. Delavelle Brachial plexus and tractography (DTI) Poster Nr 47	81
A.Y. Vasiliev, N.S. Serova, A.I. Ushakov Intraoperative control of dental implantation with digital microfocal radiography Poster Nr 48	82
M.V. Vykluk, A.Y. Vasiliev, I.N. Gipp Difficulties in differential diagnosis of head and neck cystous formation Poster Nr 49	83
C. Waldherr, A. Christe, P. Zbären, E. Stauffer, H.C. Thoeny MRI of parotid tumors: typical lesion characteristics in MR improve discrimination between benign and malignant disease Oral presentation	84

Buccal space revisited ? A guided tour through the buccal space

P. Alves, A. Borges

Hospital de S.José-CHLC; IPO-Francisco Gentil, Lisbon, PT

Poster Nr 1

Objective:

To illustrate the normal radiological anatomy and imaging spectrum of pathological conditions of the buccal space with emphasis on cross sectional imaging studies (CT and MRI), and to correlate the imaging characteristics with the most important pathological features.

Materials and methods :

A retrospective review of head and neck imaging examinations was conducted and cases displaying buccal space lesions were selected. Images were then retrieved, along with the patient's clinical information and histopathological reports. Cases with salient imaging features were selected in order to provide an educational pictorial review.

Results :

The buccal space is an anatomical compartment anterior to the masticator space, external to the buccinator muscle, and in close relationship with the mandible, the parotid and submandibular spaces. In addition to fat tissue, that makes up for the bulk of this space, its main components are muscles involved in facial expression, the parotid duct, an accessory parotid when present, small salivary glands, neurovascular structures and lymph nodes. Pathological processes can originate from each of these components or reflect an extension of lesions from neighboring spaces and examples of these are displayed in this pictorial review with a brief discussion of the most important imaging characteristics for each case.

Conclusion :

Even though pathological conditions affecting the buccal space are more accessible to clinical examination than other neck compartments, imaging still plays an important role in suggesting an origin and defining the anatomical extent of the changes encountered. A knowledge of the normal radiological anatomy of the buccal space along with the most common pathological conditions is important for the radiologist involved in interpreting head and neck studies in order to provide a working differential diagnosis for the referring clinician and to help in pre-surgical planning when an intervention is being contemplated.

Inflammatory myofibroblastic tumor of the nasal cavity in a 6 year old child

M. Anooshiravani, R. Kohler, B. Pittet, B. Rillet, M. Becker

Pediatric Radiology, Hôpital Cantonal de Genève

Poster Nr 2

Objective :

To describe the radiological findings (CT, MRI, angiography) of a rare tumor of the head and neck region in a pediatric case.

Materials and methods :

A six year-old african girl presented with a large mid facial mass occupying the nasal cavity, causing severe hypertelorism, destruction and remodelling of bony structures of the skull.

Results :

She underwent CT and contrast-enhanced MRI on admission. The patient also underwent X-ray angiography demonstrating hypervascularization of the mass, which was then embolized. Biopsies revealed an inflammatory myofibroblastic tumor (IMT). A few days later surgical resection was performed. The characteristic imaging features of this rare entity are described in detail in the poster.

Conclusion :

Inflammatory myofibroblastic tumor is a benign, invasive lesion of the soft tissue and viscera in children. Head and neck location of the tumor is very rare and presurgical diagnosis is difficult because of diverse radiological manifestations.

Comparison of conventional and MR sialography with clinical correlation in benign salivary gland disease

J. Aw, M.E. Williams, V.Beric

Frenchay Hospital, North Bristol, Bristol, UK

Poster Nr 3

Objective :

Conventional sialography is the current gold standard for investigation of benign salivary gland disease. We present a prospective study of 22 patients who underwent sequential conventional and MR sialograms and report the findings.

Materials and methods :

Prospective study of 28 patients who, following assessment in a maxillofacial clinic were referred for salivary gland imaging for suspected benign salivary duct disease. All patients underwent MR imaging of the salivary glands using heavily T2 weighted sequencesconventional sialography of the suspected duct followed by conventional sialography of the suspected duct. The MRI images were not reviewed prior to the conventional sialogram. The two modalities were then compared by two observers. The patients notes were subsequently reviewed for clinical outcome.

Results :

There was good correlation of findings between the two modalities with respect to calculi and strictures. We were unable to cannulate the duct in 3 patients so in these patients the only imaging was by MRI. Similarly 2 patients were too claustrophobic to tolerate the MRI scan. MRI demonstrated additional findings in 6 patients including abnormal lymph nodes and pathology in other salivary glands.

Conclusion :

Good correlation between the clinical and imaging findings and between the two imaging modalities. In patients with difficult duct cannulation or claustrophobia the other technique can be used with a high degree of confidence.

Physiological and benign causes of F-18 fluorodeoxyglucose (FDG) uptake within the head and neck on PET/CT imaging

J. Aw, J. Searle, G. McGann, I. Hagan, E. Brown, I. Lyburn

Royal College of Radiologists, Cheltenham Imaging Centre, London, UK

Poster Nr 4

Objective :

FDG PET/CT role in Head & Neck malignancy is in diagnosis, staging & follow up. Increased FDG uptake is not limited to malignant disease. We present a pictorial review of physiological & benign causes of increased FDG uptake in extracranial H&N imaging.

Materials and methods :

A retrospective review of all cases referred to the South West regional referral centre for PET/CT imaging over a period of 1 year was performed. We identified cases of normal physiological uptake of F-18 fluorodeoxyglucose (FDG) in the Head & Neck region. Benign causes of increased uptake were also identified.

Results :

The review of imaging with subsequent clinical correlation, demonstrated a high incidence of non-malignant uptake. These findings are illustrated with respective examples.

Conclusion :

There are a wide variety of physiological and benign causes of increased FDG uptake within the head and neck. An appreciation of these potential pitfalls is invaluable to the radiologist when interpreting Head & Neck PET/CT to avoid misinterpretation.

Beware: the salivary gland pseudomass

D.J. Bell, T. Beale

Department of Radiology, Royal National Throat, Nose and Ear Hospital, London, UK

Poster Nr 5

Objective :

To describe and illustrate the normal anatomy of the submandibular and sublingual glands and both the common and rare anatomical variants demonstrating the clinical relevance of these variants.

Materials and methods :

The mylohyoid muscle acts as a sling supporting the floor of mouth. In the majority of individuals there are congenital defects in the anterior portion of this muscle. In some cases the sublingual gland herniates through these defects, forming a mylohyoid bouton; a pseudomass that can produce clinical confusion. This herniated gland may be the origin of an atypical ranula presenting as an anterior submandibular space mass. More rarely aplasia of the submandibular gland is seen; this is often associated with syndromes although sporadic cases are also seen. By contradistinction the presence of accessory submandibular glandular tissue is distinctly unusual.

Results :

The normal anatomy of the submandibular and sublingual glands will be demonstrated on ultrasound and cross-sectional imaging. A wide variety of cases will then be used to illustrate the imaging appearances of the common and rare anatomical variants of these salivary glands. Examples of the atypical ranula arising from the herniated sublingual gland will be demonstrated and compared with the commoner floor of mouth and plunging ranulas.

Conclusion :

The purpose of this pictorial review is to familiarise the reader with both the common and unusual anatomical variants of the submandibular and sublingual glands highlighting the clinical ramifications of these anatomical variations.

The CT appearances of normal and abnormal craniofacial topographical anatomy

D.J. Bell, S.E.J. Connor

Department of Radiology, Guy's Hospital, London, UK

Poster Nr 6

Objective :

- 1.To learn the normal 3D surface anatomy of the eyes, external ear, nose, lips and associated facial structures with the help of volume reconstructed multislice CT.
- 2.To appreciate the 2D planar correlates of this anatomy on reconstructed CT scans.

Materials and methods :

Cross sectional imaging is principally required to complement clinical examination by assessing the deeper craniofacial structures. When describing the clinical appearances of lesions and abnormalities related to the eyes, ears, nose or lips, clinicians frequently use surface anatomical terms which are less familiar to the radiologist. Contemporary imaging allows us to view and describe the topographical changes in surface facial anatomy occurring in disease.

Results :

We shall illustrate the normal three-dimensional anatomy of these regions on volume reconstructed multislice CT and demonstrate the corresponding locations as on planar cross-sectional imaging. We will then illustrate how understanding these anatomical terms helps describe craniofacial pathologies such as congenital craniofacial anomalies and skin carcinomas. This improves the ability of the radiologist to relate the clinicians' findings in superficial structures to the imaging appearances of deeper structures allowing accurate descriptions and dialogue with the referring clinician.

Conclusion :

This exhibit will permit the radiologist to understand and describe craniofacial topographical anatomy on CT so aiding radiological descriptions and correlation with superficial clinical findings.

Multidetector CT in the investigation of vocal cord palsy

D.J. Bell, E.K. Woo

Department of Radiology, Guy's Hospital, London, UK

Poster Nr 7

Objective :

To describe and illustrate the anatomy of the nerves that supply the vocal cords and the CT appearances of different pathology that can cause vocal cord palsy.

Materials and methods :

Vocal cord paralysis is a relatively common clinical problem that can occur from pathology arising at any point along the course of the recurrent laryngeal or vagus nerves. Patients usually present with symptoms of a hoarse voice and paralysis is confirmed by direct visualisation of the vocal cords.

The role of imaging is to examine the entire course of the recurrent laryngeal and vagus nerves to establish the site and cause of the nerve palsy.

Results :

In this poster we describe the anatomy of the vagus and the recurrent laryngeal nerves and the extralaryngeal CT appearances of different aetiology of the vocal cord palsy. Skull base lesions (vagal schwannomas, glomus vagale, malignancy), cervical lymphadenopathy (squamous cell carcinoma, tuberculosis, lymphoma), thyroid lesions (carcinoma, retrosternal goitre), mediastinal lesions (adenopathy from lung carcinoma, nodal disease from breast carcinoma, oesophageal carcinoma and thoracic aortic aneurysm) will be discussed and illustrated. Pathological correlation will be provided.

Conclusion :

The purpose of this exhibit is to familiarise the reader with the anatomy of the vagus and recurrent laryngeal nerves and to give a pictorial review of the common pathologies that present with vocal cord paralysis.

Rhinolithiasis

D.J. Bell, S.E.J. Connor

Department of Radiology, Guy's Hospital, London, UK

Poster Nr 8

Objective :

To describe and illustrate the clinical and radiological features of the rhinolith, a rare and poorly recognised lesion of the nasal cavity.

Materials and methods :

Rhinolithiasis is a rare and under-diagnosed clinical entity. It is typically found incidentally in patients presenting with unilateral rhinological symptoms. These include nasal obstruction, facial pain, purulent rhinorrhoea and epistaxis. The pathogenesis of the condition is poorly understood but it is likely that these small calcified lesions form around foreign bodies or endogenous materials. Occasionally the presence of rhinoliths can precipitate a rhinitis leading to potentially more serious complications such as polyposis, sinusitis, and even, septal perforation. Imaging has an important role in diagnosing this condition, excluding complications and in pre-surgical planning.

Results :

In this exhibit we will review the clinical presentation and radiological appearances of rhinolithiasis. Since 2003 there have been 5 confirmed cases of this rare condition at our institution. We shall compare and contrast the imaging findings of the cases and correlate with their clinical, surgical and pathological features. Moreover we will review the current literature regarding this unusual disease entity.

Conclusion :

We hope that having reviewed this poster the reader will have a better appreciation and understanding of this rare disease entity.

Dynamic ocular MRI- comparison of clinical testing and imaging

B.I. Berg-Boerner, C. Kunz, K. Schwenzer-Zimmerer, E.W. Radü, C. Kober, K. Scheffler, C. Buitrago-Téllez, A. Palmowski-Wolfe

Universitätsspital Basel, Wiederherstellende Chirurgie Kiefer- u. Gesichtschirurgie, Basel, CH

Poster Nr 9

Objective :

In this study near real time MRI, a technique for the recording of eye movements was qualitatively evaluated and quantitatively compared with clinical testing.

Materials and methods :

Eye movements of 22 patients were tracked in the horizontal and vertical plane. In all cases, diplopia was the inclusion criteria. A standard 1.5 T MRI with a TrueFISP sequence (180ms/image, 1.3x1.3 mm spatial resolution) was used. The average slice thickness was 5 mm. The average acquisition time for one sequence was about 10 sec. The eye movement was assessed in two planes (sagittal and axial). Three independent physicians graded the visibility of extraocular muscles qualitatively throughout the movement. For the clinical evaluation, maximal monocular horizontal and vertical excursions measured in mm according to Kestenbaum with a see-through ruler held over the patient's eye were compared to the angle of the largest possible eye movements in the MRI sequence (in degrees measured on print-outs) by using the Pearson test.

Results :

A distinction could be made between mechanical adhesions from entrapment and paralytic eye movement disorders. Three independent assessors graded the MRI quality (from 1= not visualized to 5 = very good quality, continuous visualization). According to the plane examined, visualization was better for the horizontal and vertical rectus muscles than for the superior and inferior oblique. Complete visualization throughout the axial or sagittal sequence varied between about 10% and 90% respectively. MRIs with complete visualization were compared to the clinical measurements. Positive correlations were found between the angles measured in the MRI and complete movement of the right eye, between complete movement of the left eye as well as for the upwards-downwards movement of the right eye.

Conclusion :

The oculodynamic MRI promises to be a very helpful tool for the maxillofacial surgeon and ophthalmologist. With a good correlation to clinical findings, the oculodynamic MRI can record and visualize normal and pathologic ocular movements. Its potential application is particularly in the setting of preoperative planning of posttraumatic diplopia or periorbital tumors with secondary ocular motility disorders.

Outcome prediction after surgery and chemoradiation of squamous cell carcinoma in the oral cavity, oropharynx and hypopharynx: perfusion CT parameters versus tumor volume

S. Bisdas, M.G. Mack, G. Glavina, K. Surlan-Popovic, T.J. Vogl, Z. Rumboldt

Department of Radiology, Johann Wolfgang Goethe University, Frankfurt, DE

Oral presentation

Objective :

To assess whether pre-treatment perfusion CT (PCT) may predict outcome in chemoradiated patients with oral cavity, oropharynx, and hypopharynx squamous cell carcinoma (SCCA) after surgical excision.

Materials and methods :

Twenty-one patients with SCCA were examined before treatment. The primary site was oral cavity in 6, oropharynx in 7, and hypopharynx in 8 patients; there were eleven T2, six T3 and four T4 tumors. PCT was performed at the level of largest tumor diameter based on standard neck CT. The data was processed to obtain blood flow (BF), blood volume (BV), mean transit time (MTT), and permeability surface area product (PS). Regions of interest were free-hand positioned on the lesions to obtain PCT measurements. Tumor volume was also calculated. Follow-up was performed with PET/CT and endoscopy. Pearson correlation coefficient was used for comparison between the subgroups. A regression model was constructed to predict recurrence based on the following predictors: age, gender, tumor (T) and nodal (N) stage, tumor volume, and PCT parameters.

Results :

BFmean, BFmax, BVmean, BVmax, MTTmean, PSmean, and PSmax were significantly different between patients with and without tumor recurrence (0.0001)

Conclusion :

Our data suggest that PCT parameters have a predictive role in patients with SCCA oral cavity, oropharynx, and hypopharynx squamous cell carcinoma (SCCA) after surgical excision and chemoradiation.

Tissue perfusion and glucose metabolism coupling in head and neck squamous cell carcinomas using combined PET/CT imaging

S. Bisdas, Z. Rumboldt, K. Spicer, T.J. Vogl, M.G. Mack

Department of Radiology, Johann Wolfgang Goethe University, Frankfurt, DE

Oral presentation

Objective :

To examine the relationship between perfusion measurements derived from perfusion CT (PCT) and glucose standardized uptake values (SUV) in head and neck squamous cell carcinomas (SCCAs) using PET/CT imaging.

Materials and methods :

Twenty-five primary and recurrent SCCAs were prospectively evaluated using combined PET/CT. SUVmean, SUVmax, blood flow (BF), blood volume (BV), mean transit time (MTT), and permeability (PS) values were calculated using manually drawn ROIs over the lesions and the healthy muscle tissue. Parametric comparison tests, correlation coefficients, and regression analysis were performed.

Results :

The mean (\pm SD) SUVmean, SUVmax, BF, BV, MTT, and PS values in the tumor tissue were 6.26(\pm 1.48), 15.25(\pm 3.81), 91.50(\pm 24.69), 5.08(\pm 1.17), 7.51(\pm 2.24) and 23.08(\pm 8.77), respectively. All PET/CT and PCT parameters of muscle versus tumor tissue were statistically different (0.0001).

Conclusion :

Tissue perfusion-metabolic coupling is evident in head and neck SCCAs and may provide additional information for the tumor function in patients undergoing PET/CT studies.

Prediction of tumor response and recurrence in advanced squamous cell carcinoma of the oropharynx: The use of pre-treatment dynamic contrast-enhanced CT microcirculatory parameters versus tumor volume

S. Bisdas, Z. Rumboldt, M. Baghi, J. Wagenblast, K. Surlan-Popovic, T.J. Vogl, M.G. Mack

Department of Radiology, Johann Wolfgang Goethe University, Frankfurt, DE

Poster Nr 10

Objective :

To assess whether pre-treatment dynamic contrast-enhanced CT (DCE-CT) and tumor volume may predict response to induction chemotherapy and to short-term local tumor control of advanced squamous cell carcinoma (SCCA) in oropharynx.

Materials and methods :

Nineteen patients with SCCAs underwent a pre-treatment DCE-CT, contrast-enhanced CT (CECT), and conventional endoscopy. After induction chemotherapy, tumor response was determined according to RECIST criteria. The responders as well as the non-responders underwent conventional follow-up endoscopies to detect any recurrence. The DCE-CT parameters, the tumor volumes (based on CECTs), the radiological response rates, and the survival data were analyzed using Cox-proportional hazards model, Receiver Operating Characteristic (ROC), and Kaplan-Meier analysis.

Results :

The pretreatment tumor volume was 74.9 ± 13.5 ml, the postinduction volume was 38.0 ± 17.3 ml. Eleven patients were responders. The baseline blood flow (BF), blood volume (BV), and permeability surface area product (PS) in the responders were significantly higher while mean transit time (MTT) was significantly lower in the responders than in the non-responders ($p < 0.002$). DCE-CT variables were correlated with postinduction tumor volume ($r = 0.46$, $p < 0.001$). The progression free survival (PFS) (in months) of responders was 11.2 ± 5.5 and of non-responders 10.5 ± 6.5 ($p = 0.8$). The pretreatment tumor volume was correlated with the PFS in the pooled patients group ($r = 0.4$, p

Conclusion :

Tumor volumetric and BF values may predict PFS in patients with advanced SCCA in the oropharynx. Pre-treatment DCE-CT derived parameters may predict response after induction radiochemotherapy while did not hold any predictive value for the post-induc

The utility of whole organ macrosection technique in the management of head and neck tumors and its correlation to preoperative imaging

M. Bongiovanni, P. Dulguerov, A. Lobrinus, K. Burkhardt, M. Gremaud, M. Becker

Service de Pathologie Clinique, Hôpitaux Universitaires de Genève, Genève, CH

Poster Nr 11

Objective :

The aim of this poster is to present the utility of the whole organ large histologic sections (LHS) technique on the management of head and neck (H&N) tumors and to correlate it with pre-operative CT and/or MRI.

Materials and methods :

All H&N neoplastic cases processed with the LHS technique were selected from the files of our department from 2003 to 2007. In all cases the entire specimen, oriented according to the surgeon's indication, was cut into transverse sections, formalin fixed and embedded into large paraffin blocks. If bone tissue was present, classic bone decalcification was performed. 5-mm hematoxylin-eosin stained sections were obtained. Clinico-pathological parameters were registered for each case: type of surgical intervention, histological type, multifocality, status of the resection margins, pTNM and presence of preoperative radiological imaging (CT and/or MRI).

Results :

A total of 51 tumors were identified. Patients were 48 male and 3 female (43-81 years, mean 60.72). Forty-two cases were pharyngolaryngectomies/laryngectomies, 6 mandibulectomies (complete or partial) and 1 maxillectomy, partial glossectomy and pharyngectomy. Tumors consisted of squamous cell carcinomas (n=43), thyroid carcinomas (n=2) and post-radio and/or chemotherapy lesions (n=6). Multifocality was detected in 7 cases and a positive resection margin in 15. Pathological TNM classification comprised pT4 any N Mx (n=22), pT3 any N Mx (n=6), pT2 any N Mx (n=5), pT1 any N Mx (n=3), R1 (n=2) and R2 (n=7).

Conclusion :

The LHS technique allows the radiologist to correlate pre-operative CT and/or MRI with histology, improving his diagnostic skills and provides detailed information that can aid the oncologist in selecting the best treatment.

The spectrum of imaging findings of ingested gastrointestinal foreign bodies

K.M. Chew, J.P.N. Goh

Singapore, SG

Poster Nr 12

Objective :

To describe the spectrum of imaging findings of ingested gastrointestinal foreign bodies.

Materials and methods :

A review of all radiologic examinations (CT, barium swallow) for cases of ingested foreign bodies from 2005- 2007 in the Diagnostic Radiology Department was performed. The types of foreign bodies, locations of lodgment and associated complications were recorded. Interesting cases with specific teaching points were collected with subsequent detail analysis of the radiologic findings, and correlation made with the procedural reports of all patients who subsequently underwent endoscopy and surgery. A literature review on the radiological evaluation of ingested foreign bodies was also performed.

Results :

Foreign body ingestion is common in our population, with fish and other meat bones being the most commonly ingested. The oesophagus was the most common site of foreign body lodgment, followed by the stomach. Potential complications varied depending on the location, and foreign body type. A wide spectrum of imaging findings ranging from mucosal lacerations to fatal mediastinitis and peritonitis has been reported. Although plain radiographs are commonly used for initial surveys, their sensitivity and specificity were less than satisfactory, as vascular, cartilaginous and soft tissue calcifications may mimic the appearance of foreign bodies. Radiographic contrast studies were the modality of choice in the past decade. However, computed tomography has gained popularity amongst the clinicians in our institution due to its easy availability, high sensitivity and specificity, and ability to provide detailed anatomical information, as well as complications related to ingested foreign bodies.

Conclusion :

Radiological studies are vital in the management of ingested gastrointestinal foreign bodies. Comprehensive reports on types and locations of foreign bodies are invaluable in the removal of foreign bodies and hence prevention of major complications.

CT and MRI cochlear diameter measurements may predict electrode length to 360 degrees insertion depth angle

S.E.J. Connor, D.J. Bell

Neuroradiology Department, Kings College Hospital and Radiology Department, Guy's and St Thomas' Hospital, London, UK

Oral presentation

Objective :

To establish whether the distance between the round window and the lateral cochlear wall on CT or MRI may be used to predict the length of cochlear implant array required to be inserted to the 360 degrees point of the basal turn.

Materials and methods :

Post operative temporal bone CT and preoperative temporal bone MRI data was studied for 18 paediatric patients undergoing "straight" cochlear array implantation. For both the CT and MRI studies, a double oblique paracoronal reformatted (MIP/MINIP) image was obtained and distances measured between the round window and lateral cochlear wall. The measurements were recorded by two independent radiologist observers on two occasions. Adjusted distance measurements were applied to a spiral function equation in order to estimate the length of electrode array extending between the round window entry point and the 360 degrees point. This was compared with measurements of implant length to this insertion depth on post operative CT. The precision (intra-and inter-observer reproducibility) of CT and MRI cochlear distance measurements was calculated. Accuracy of CT and MRI measures of the cochlear distance in predicting the 360 degrees point insertion depth implant length was determined.

Results :

Intraobserver reproducibility (CT/MRI) for each of the 2 observers was $r(\text{Pearson})=0.85/0.87$ and $r=0.56/0.67$. Interobserver reproducibility (CT/MRI) was $r(\text{Pearson})=0.69/0.84$. There was no bias between CT and MRI measurements with a mean difference of

Conclusion :

CT and MRI measures of cochlear diameter predicted implant insertion depths to 360 degrees which were approximately 1mm greater than the actual length. MRI measurements were slightly more accurate and precise than those obtained with CT.

Diagnostic accuracy of DWI ?MRI for discrimination of cervical metastatic lymph nodes in head and neck squamous cell carcinoma

R.B.J. de Bondt, M.C. Hoerberigs, P.J. Nelemans, W. Deserno, J.W. Casselman, J. Verwoerd, B. Kremer and R.G.H. Beets-Tan

Department of Radiology, Maastricht University Medical Center, Maastricht, NL

Oral presentation

Objective :

To determine the accuracy of diffusion weighted imaging (DWI) for discriminating malignant from normal cervical lymph nodes in head and neck squamous cell carcinoma (HNSCC).

Materials and methods :

A total of 219 lymph nodes (26/219 metastases) in 16 consecutive patients with HNSCC were evaluated on MRI (1.5 Tesla). Apparent Diffusion Coefficient (ADC) values were calculated by using two b-values (0 and 1000 s/mm²). Two readers evaluated all lymph nodes for short axial diameter, morphological criteria (borders and heterogeneity on T2-WI) and ADC values. Lymph nodes were matched to the histopathological results based on location and size per neck level. The optimal threshold for ADC value was determined. Univariate and multivariate logistic regression analysis - sensitivities, specificities and diagnostic odds ratios (DOR) and ROC with Area Under the Curve (AUC) and Confidence Interval (95%CI) - were performed.

Results :

With an ADC threshold of 1000×10^{-6} mm²/sec, sensitivity and specificity were 92.3% and 83.9% (DOR=62.7), and NPV 98.7% (162/164). Sensitivity and specificity of border-criteria (61.5% and 98.3%) and T2-heterogeneity (50% and 94.8%) were significantly lower. The AUC for ADC was 0.90 (95% CI 0.84-0.98) and for size and morphological criteria together 0.91 (95% CI 0.84-0.98). When taking all morphological and ADC together, the AUC was 0.9 (95% CI 0.97-0.99).

Conclusion :

DWI alone is comparable to size and morphological criteria together in predicting malignant lymph nodes. The addition of ADC measurements to the conventional criteria significantly improves the detection of malignant lymph nodes in patient with HNSCC.

An unusual iatrogenic unilateral fracture of the coronoid process of the mandible that was not diagnosed for 12 years by both radiologists and dentists

A. Delantoni

Aristotle University of Thessaloniki, Thessaloniki, GR

Poster Nr 13

Objective :

To present an unusual case of an isolated unilateral fracture of the coronoid mandibular process that occurred during surgery and was not observed by the radiologists

Materials and methods :

The mandible is reported as the most commonly fractured facial bone in trauma cases. The reports on fractures of the coronoid mandibular process however are rare in occurrence. The incidence of coronoid process fractures vary according to various authors from 1% to 2.1% and they are the lowest in occurrence of all mandibular fractures despite the fact that the mandible is the most commonly fractured facial bone. Bearing in mind that the majority of fractures of the coronoid process are bilateral, the percentile of unilateral coronoid process fractures is very limited. In the majority of cases the fractures are caused by trauma or automobile accidents, with hardly any mention to other causes in the literature. The case presented is an iatrogenic unilateral fracture of the coronoid process of the mandible that was not diagnosed for over 15 years.

Results :

The CT examination revealed a transverse fracture of the coronoid process of the mandible without significant displacement of the fractured segment. The three dimensional reconstruction images showed the exact location of the fractured segment in space and its slight medial location.

Conclusion :

The significance of careful observation of radiographs and history of the patient by radiologists and doctors is given. A thorough clinical and radiographic evaluation is necessary prior to treatment but in many cases it is not undertaken properly.

Aural lesions imaging, the tip of the iceberg

A.H El Beltagi, K. El Sebeih, N. El Shemari, L. Al Rabiaa

Al Sabah Hospital Radiology and ENT department, Ministry of health, Kuwait, KW

Poster Nr 14

Objective :

aural lesions, are a frequent presentation to the Ear Nose and Throat (ENT) clinic. Most of these are polyps related to inflammatory disease in the middle ear. This pictorial review demonstrates different pathologic entities of aural lesions.

Materials and methods :

over the past 10 years, lesions presenting with aural lesions either polyps in the EAC, auricular and periauricular swelling, stenosis, or discharge in Al Sabah Hosp Kuwait- ENT department, were evaluated with computed tomography pre- and post intravenous injection of iodine based contrast, and or magnetic resonance imaging

Results :

Congenital aural lesions included: congenital cholesteatoma, First branchial cleft cyst and sinus. Traumatic cephalocele. Inflammatory lesions included keratosis obtrons, granular myringitis, necrotizing otitis externa, mycobacterial tuberculosis, langerhan cell histiocytosis, Wegener's granulomatosis, and post radiation fibrosis. Neoplastic lesions, included benign lipoma, osteoma, exostosis, fibrous dysplasia, paraganglioma, facial nerve neuroma, neurofibroma and meningeoma. Malignant neoplasia include squamous cell carcinoma, ceruminous adenocarcinoma, and rhabdomyosarcoma

Conclusion :

For lesions readily available to inspection in the EAC, the radiologist approach, is to deal with the lesion as tip of an iceberg, and to assess its deeper extent. Specific imaging appearances of certain lesions can provide specific diagnosis.

Agensis of the sphenoid sinus

G. Gavridakis, E. Astropekaki, E. Manolakakis, S. Stagkouraki, G. Liodakis, K. Psaras, N. Syrmos, L. Triantafyllou

Department of Computed Tomography, Venizelion Hospital, Heraklion, GR

Poster Nr 15

Objective :

We present 4 cases of agensis of the sphenoid sinus, discovered by chance during a multislice CT scan of the head

Materials and methods :

In total 921 multislice CT exams of the head (paranasal sinuses and temporal bones) were examined in our CT department from May 2005 until March 2008.

Results :

Agensis of the sphenoid sinus was discovered in 4 of the cases (0,43%). Two of the patients were referred for a CT scan because of symptomatology from the nose and paranasal sinuses with one of them having a history of thalassemia. From the other two patients one had a history of headaches and the other unilateral reduction of his vision.

Conclusion :

The sphenoid sinus absence is extremely rare. Pneumatisation of the sphenoid sinus is potentially important in the planning of a trans-sphenoidal hypophysectomy.

Pharyngeal wall bulging. What we found behind it

A. Germano, I. Cravo, T. Palma, E. Serrão, G. Alves

Hospital Fernando Fonseca. Radiology Department, Neuroradiology Unit, ENT department, Porto Salvo, PT

Poster Nr 16

Objective :

Pharyngeal wall bulging is a frequent indication for demand of an urgent CT examination of the neck. Our purpose is to present the iconography of both the rare and most frequent pathologies found.

Materials and methods :

A retrospective study, covering neck CT examinations, recorded between May 1, 2006 and May 31, 2008, will be reported. All the CT examinations were requested by the emergency department and had the clinical information of pharyngeal wall bulging.

Results :

148 urgent CT exams of the neck were requested. 72 of the 148 exams had clinical information of pharyngeal wall bulging. The following causes of pharyngeal wall bulging were identified: 63 patients had inflammatory/infectious conditions including necrotic retropharyngeal adenopathy, oedema, retropharyngeal, parapharyngeal and tonsillar abscesses; 4 patients had tumours, mainly nerve sheath tumours and paragangliomas; 2 patients presented an ectatic carotid artery; 1 patient suffered from longus colli tendonitis.

Conclusion :

Inflammatory/infectious conditions are the most frequent causes of pharyngeal wall bulging. Imaging is a useful tool for the differential diagnosis and therapeutic decision.

Use of high-resolution variability in the orientation of the osseous spiral lamina along the basal turn of the cochlear in twenty normal hearing individuals ? A potential role prior to cochlea surgery

D. Gibson, A. Whyte, S. Karamfiles, M. Atlas

Perth radiological Clinic, Perth, AU

Oral presentation

Objective :

Using high-resolution T2 driven equilibrium radio frequency reset pulse (DRIVE) sequences from twenty normal hearing patients, we sought to define the inter-subject variability in the orientation of the osseous spiral lamina (OSL) at the cochlea hook region and along the basal cochlea turn.

Materials and methods :

The magnetic resonance temporal bone studies of twenty consecutive normal hearing individuals were retrospectively reviewed. The imaging was requested for a variety of symptoms following clinical assessment and audiology testing. Sensorineural hearing loss on the side of interest led to patient exclusion. High-resolution T2W DRIVE sequences were acquired on a 3T Philips Achieva scanner. The sequence parameters were: repetition time 5.5ms; echo time 2.8 ms; field of view 15 x 15 cm; flip angle 100; matrix size 512 x 512; slice thickness 0.75mm. Acquisition time was 3 minutes and 38 seconds. Fat-suppressed images were obtained with a Spectral Attenuated Inversion Recovery technique. Sequences were acquired in the axial plane using an 8-channel SENSE head coil. Three dimensional models of the cochlea were generated using a GE workstation. To mimic the trajectory used in cochlea electrode deployment, we reconstructed images in an oblique sagittal plane and proceeded anteriorly away from the round window membrane (RWM), moving along the basal turn of the cochlea. Angular measurements of the OSL were made at 1, 3, 5 and 7mm distal to the most posterior margin of the RWM.

Results :

Data was collected retrospectively from ten right and ten left audiotically normal labyrinths. All angular measurements were made by consensus viewing (DG/SK). Our patient group ranged in age from 24 to 79 years (mean; 51). The male to female ratio was 1:1. Posteriorly viewed along an oblique sagittal plane, incrementally moving along the basal turn of the right cochlea, the OSL progressively rotates in a clockwise direction, passing through a vertical orientation. Mirroring this, along the basal turn of the left cochlea, the OSL rotates through the vertical plane in an anti-clockwise direction. Over a distance of seven millimetres, the average clockwise rotation on the right OSL is 28 degrees. The average counter-clockwise rotation of the left OSL is 23.5 degrees. On both sides, the rotation of the OSL was unequal along its own axis with the greatest incremental increase in rotation occurring between one and three millimetres beyond the RWM (R=17°, L=9.5°). The smallest increment was between five and seven millimetres along the basal turn with 3.1 degrees of rotation on the right and 3.5 degrees of rotation on the left.

Conclusion :

Employing T2W sequences and an oblique sagittal plane, we simulated the approach used in cochlea implantation. Incrementally proceeding along the basal turn of both cochleae, there was a mirrored uneven, progressive clockwise (R) and counter-clockwise (L) rotation of the OSL on its own axis.

Diagnostic adequacy of ultrasound guided fine needle aspiration cytology in neck lump investigation: a comparative audit of three reporting setups

Y. Gupta, N. Stephens, T. Beale

Royal National Throat, Nose & Ear Hospital, London, UK

Oral presentation

Objective :

There is little data on the effect of reporting setups on ultrasound guided FNAC results. We examined whether there was a difference in the adequacy and accuracy of cytology results between three centres with different reporting protocols.

Materials and methods :

We retrospectively examined the records of all patients who underwent ultrasound guided FNAC of a head & neck mass at three radiology departments between May 2007 and May 2008. All the FNA procedures were performed by one head & neck radiologist using identical techniques and equipment at all three centres. FNAC samples from centre A were sent to one of two specialist Head & Neck (H&N) cytopathologists; almost all the samples from centre B were reported by one of three specialist H&N cytopathologists; samples from centre C were reported by one of seven available consultant pathologists/cytologists, not all of whom had a H&N interest. We examined the US and cytology reports, collecting demographic data, noting inadequate FNA results and correlating with histopathology where available.

Results :

Over 500 ultrasound guided FNAC samples were taken during this period. There was a significant difference in the adequacy rate when the FNAC was assessed by a specialist H&N cytopathologist (96% and 94% adequacy at centres A & B) as compared to a general cytopathologist (80% at centre C). Unsurprisingly the best service to the patient is when the ultrasound guided FNAC sample is reviewed by a named cytopathologist with a particular expertise and subspeciality interest. When a specified individual reports the sample a clinical relationship is established between radiologist and cytopathologist. This allows inadequate and interesting samples to be reviewed, and clinical details and techniques can be discussed.

Conclusion :

The results of this audit are being used to alter the referral pathway so that the ultrasound guided FNAC samples from centre C will be directed to cytopathologist(s) with a H&N interest. The results will then be re-audited to complete the loop.

Radiologic-pathologic correlations in complicated cases of head and neck tuberculosis

H. Haba

Univ. of Medicine, Iasi, RO

Poster Nr 17

Objective :

To evaluate with computed tomography (CT) and ultrasound (USG) complicated cases of head and neck tuberculosis in order to detect more lymph nodes, and to study their lesions.

Materials and methods :

31 patients with head and neck tuberculosis previously proved bacteriologically or histopathologically, on anti-tuberculosis treatment, presenting complications were taken for study. Each case with tuberculous nodes was subjected to ultrasound and computed tomography of head and neck area. Based on USG and CT findings, patients were subjected to repeated fine needle aspiration cytology of involved lymph node or drainage of pus.

Results :

On USG, all lesions were hypoechoic and showed necrosis. Other findings were: sharp margins in 80.4 %, hilum in 19.6 %, and abnormal surrounding tissue in 87 %, matting in 37 %, calcification in 29 % and posterior enhancement in 22 % patients. On CT, the majority of neck lesions were with central low density in 16 cases, followed by large confluent low density in 7 cases, multilocular central low density in 4 and homogeneous soft tissue density in 2 patients. Necrotising granulomatous lymphadenitis was the most common diagnosis in 15 cases, followed by necrotising in 6 cases, granulomatous in 4 patients and cerebral tuberculosis in other 6 patients. In 27 patients, culture and sensitivity test for Mycobacterium Tuberculosis from lymph node aspiration was done and 12 patients were found culture positive. Out of these, 5 were found to be multi-drug resistant cases.

Conclusion :

USG and CT technique are complementary in diagnosis and management of head and neck tuberculosis. USG is better in localization of site for biopsy/FNAC procedure and drainage of pus and CT helps in better anatomical localization of all lymph nodes.

Diffusion-weighted echo-planar MRI: still a valuable tool for differentiating primary parotid gland tumors in a large patient collective ?

C.R. Habermann, C. Arndt, J. Graessner, F. Reitmeier, M. Jaehne, G. Adam

Department of Diagnostic and Interventional Radiology, University Medical Center Hamburg-Eppendorf, Diagnostic Center, Hamburg, DE

Oral presentation

Objective :

To determine the value of diffusion-weighted (DW) echo-planar (EP) magnetic resonance (MR) imaging in differentiating various entities of primary parotid gland tumors in a large patient collective.

Materials and methods :

149 consecutive patients with a suspected tumor of the parotid gland were examined with a DW EP sequence using a 1.5 T unit. ADC maps were digitally transferred to MRicro (Chris Rorden, University of Nottingham, Great Britain) and evaluated with a manually placed irregular region of interest (ROI) containing the entire tumor. Image analysis was performed by two radiologists independently and intraclass correlation coefficient was computed. Histological diagnosis was obtained in every patient. Additionally, a circular ROI containing 100?200 pixels was placed in the cerebrospinal fluid (CSF) next to the spinal cord in every patient. For comparison of apparent diffusion coefficients (ADC), paired two-tailed Student t-test with Bonferroni correction was used.

Results :

In 128 patients a primary parotid gland tumor was confirmed by histology. Among the observers a high correlation was calculated (0.98). For CSF the mean ADC value was $2.61 \times 10^{-3} \text{ mm}^2/\text{sec} \pm 0.22$ (mean \pm standard deviation) ADC values of pleomorphic adenomas ($2.09 \times 10^{-3} \text{ mm}^2/\text{sec} \pm 0.16$) were significantly higher than all other entities, except for myoepithelial adenomas ($1.86 \times 10^{-3} \text{ mm}^2/\text{sec} \pm 0.18$; $P = 0.54$). ADC values of Warthin tumors ($0.85 \times 10^{-3} \text{ mm}^2/\text{sec} \pm 0.1$) were different from myoepithelial adenomas, lipomas, and salivary duct carcinomas (P

Conclusion :

In contrast to the literature, DW MRI has only a limited value in differentiating primary parotid gland tumors in a large patient collective due to an overlap between benign and malignant conditions.

Value of apparent diffusion coefficient calculation before and after gustatory stimulation in the diagnosis of acute or chronic parotitis

C.R. Habermann, T. Ries, C. Arndt, M. Regier, J. Graessner, M.C. Cramer, F. Reitmeier, M. Jaehne, G. Adam

Department of Diagnostic and Interventional Radiology, University Medical Center Hamburg-Eppendorf, Diagnostic Center, Hamburg, DE

Oral presentation

Objective :

To investigate the value of diffusion-weighted (DW) echo-planar imaging (EPI) for quantifying physiological changes of the parotid gland before and after gustatory stimulation in patients suffering from acute or chronic recurrent inflammation in comp

Materials and methods :

Using a DW-EPI sequence at 1.5T parotid glands of 19 consecutive patients with acute (n=14) and chronic (n=5) inflammation of parotid glands and 52 healthy volunteers were examined. Magnetic-resonance (MR) images were obtained before and after gustatory stimulation with 5 cc of lemon juice.

Results :

In volunteers mean ADC values of 1.14×10^{-3} mm²/sec before and 1.2×10^{-3} mm²/sec after gustatory stimulation were observed. In acute inflammation ADC values were higher before (1.22×10^{-3} mm²/sec (p=0.006)) and after stimulation (1.32×10^{-3} mm²/sec (p

Conclusion :

DW-EPI seems to display the physiological changes of the parotid gland in patients suffering from acute or chronic inflammation and might be useful for discriminating healthy from affected glands.

Differentiation of primary parotid gland tumors: does the combination of diffusion-weighted echo-planar MRI and magnetization transfer imaging offers diagnostic improvement ?

C.R. Habermann, C. Arndt, J. Graessner, F. Reitmeier, M. Jaehne, G. Adam

Department of Diagnostic and Interventional Radiology, University Medical Center Hamburg-Eppendorf, Hamburg, DE

Poster Nr 18

Objective :

To investigate the potential of diffusion-weighted (DW) echo-planar imaging (EPI) in combination with magnetization transfer imaging (MTI) using the magnetization transfer ratio (MTR) in differentiating primary parotid gland tumors.

Materials and methods :

145 consecutive patients with suspected primary tumor of the parotid gland were prospectively examined first with a T1-weighted TSE sequence for parotid gland localization. Furthermore, a DW EPI sequence (TR 1,500 msec, TE 77 msec, field of view 250 x250 mm, pixel size 2.10 x 1.95 mm, section thickness 5 mm, b factors: 0, 500, and 1,000 sec/mm²) and a single slice T1 weighted GRE sequence in in-phase and opposed-phase technique prior and post 1 kHz-off-resonance pulse were acquired. ADC maps and MT images were digitally transferred to MRIcro (Chris Rorden, University of Nottingham, Great Britain) and evaluated with a manually placed irregular region of interest (ROI) containing the entire tumor. For comparison of the results, the two-tailed Student's t test with Bonferroni correction for multiple testing was used, based on the mean ADC values for each patient, and a P value of less than .05 was determined to indicate statistical significance.

Results :

In 129 patients fourteen different subtypes of primary neoplasms of parotid glands could be verified histologically. Based on ADC values pleomorphic adenomas were differentiable from all entities (P< 0.001) except from myoepithelial adenomas (P= .054). Using MTR these two entities were not discriminated as well (P= 0.394). DW imaging failed to differentiate Warthin tumors from mucoepidermoid carcinomas, acinic cell carcinomas and basal cell adenomas (P= 0.094 to 0.604), whereas MTI was able to differentiate Warthin tumors and basal cell adenomas (P=0.004). Additionally, DW imaging failed in differentiating myoepithelial adenomas and mucoepidermoid carcinomas from basal cell adenocarcinomas (P= 0.082; 0.569), whereas MTI was able to differentiate these entities (P= 0.032; 0.014).

Conclusion :

DW imaging has a certain potential in differentiating subtypes of primary parotid gland tumors. Combining this technique with MTI can improve the non invasive approach in differentiating primary parotid gland tumors.

Dynamic contrast-enhanced MR imaging: a reliable diagnostic tool for recurrent head and neck tumors

E. Kamel

Diagnostic Radiology, Lausanne University Hospital, Lausanne, CH

Oral presentation

Objective :

To investigate the role of Dynamic Contrast-Enhanced MR Imaging (DCE-MRI) in the follow-up of patients with head and neck tumors.

Materials and methods :

Twenty seven patients were recruited. DCE-MRI was performed as a part of regular posttherapy follow-up (n=20) or for clinical suspicion of local disease recurrence (n=7). Axial dynamic T1-weighted fat sat sequences were performed in a 3-T MR scanner for a total duration of 10 minutes after contrast administration. An operator-defined region of interest was placed in the maximal enhancement area(s) of the tumor bed in all patients. A time-intensity curve was constructed and analyzed. The time to maximal enhancement (Tmax), enhancement ratio at 3 min (ER3min), and washout ratio at 10 min (WR10min) were measured. Per-lesion DCE-MRI findings were correlated with histologic analysis or with clinical and radiological follow-up.

Results :

There was a significant difference between Tmax, ER3min and WR10min of recurrent lesions and those of posttherapy tissue remodeling (2.2 min, 19%, and 20% vs. 8.3 min, 12%, and 6%, P< 0.05). Among 12 recurrent lesions in 9 patients, DCE-MRI detected 11/12 (91%) of these foci. One false negative result was due to microscopic disease residue within post-therapy scar tissue. Two radionecrotic lesions were responsible for false positive DCE-MRI results in 2 patients. These 2 lesions were characterized by indistinguishable Tmax, ER3min, and WR10min from those of recurrent tumor foci. In the remaining 16 patients, true negative DCE-MRI findings were confirmed. Accordingly, the sensitivity, specificity, and accuracy of DCE-MRI were 91%, 89% and 90%, respectively.

Conclusion :

DCE-MRI can be integrated as a valuable tool in the diagnostic work-up of patients with or without clinical or radiological suspicion of recurrent head and neck tumors.

Ultrasonographic features of follicular variant papillary thyroid carcinoma: mimicker of a benign thyroid nodule

J.H. Kim, D.S. Kim, K.H. Chang

Department of Radiology, Seoul National University Hospital, Seoul, KR

Oral presentation

Objective :

Although follicular variant of papillary thyroid carcinoma (FVPTC) is the most common subtype after conventional PTC, its cytologic diagnosis is more difficult than conventional PTC. The purpose of this study is to determine ultrasonographic (US) features of FVPTC in addition to comparison with those of conventional PTC.

Materials and methods :

Surgically proven PTCs of 44 nodules in 40 patients with FVPTC and 74 nodules in 59 patients with conventional PTC were enrolled in this study. The following US features were evaluated and compared between the two types: nodule size, shape, margin, echogenicity, calcification, and presence of hypoechoic halo. The incidences of the ultrasonographic malignant grade were compared between the two types, with the criteria of malignant grade if even one of the following US features was present: a taller than wide shape, a spiculated margin, marked hypoechogenicity, and micro- or macro-calcification.

Results :

Ovoid to round shape (95%), smooth margin (73%), and isoechoic echogenicity (52%) were the common US features of FVPTC. The mean nodule size of FVPTC was larger than that of conventional PTC (17.70 vs. 10.53 mm, P

Conclusion :

Ovoid to round shape, isoechoic echogenicity, and smooth margin are the common US features of FVPTC. FVPTC has different US features compared with conventional PTC and may mimic a benign nodule.

To evaluate the MR features in patients with nasopharyngeal tuberculosis

J.H. Kim, M.H. Yu, K.H. Chang

Department of Diagnostic Radiology, Seoul National University Hospital, Seoul, KR

Poster Nr 19

Objective :

To evaluate the MR features in patients with nasopharyngeal tuberculosis.

Materials and methods :

Seven consecutive patients (6 women and 1 man; age range, 22~68 years; mean age, 43 years) with histopathologically proven nasopharyngeal tuberculosis were enrolled in this retrospective study. MR analysis was done for the shape, signal intensity, and enhancement pattern of the lesion with the application of the tumor-node classification of nasopharyngeal carcinoma by American Joint Committee on Cancer.

Results :

The nasopharyngeal lesions showed two patterns of shape, infiltrative wall thickening (n=6) and a discrete polypoid mass (n=1). In all cases, they showed intermediate signal intensities on T1 and T2 weighted images with homogeneous enhancement on enhanced-T1 weighted images. Characteristically, 6 out of 7 patients showed nonenhancing superficial T2 bright signal intensity over irregular mucosal lesion, which were considered as ulcerative mucosal changes on clinico-radiological correlation. The applied TN classifications for the 7 patients with nasopharyngeal tuberculosis included T1N1 (n=2), T2N0 (n=3), T3N0 (n=1), and T4N1 (n=1).

Conclusion :

Although nasopharyngeal tuberculosis presents like variable stages of nasopharyngeal carcinoma, the common MR findings of infiltrative wall thickening, indeterminate signal intensities on T1 and T2 weighted images with strong enhancement, and nonenhancing superficial T2 bright signal intensity over irregular mucosal lesion may be helpful for differentiating nasopharyngeal tuberculosis from nasopharyngeal carcinoma.

Preoperative thyroid cancer staging: what the radiologist should know

S.J. Kim

Diagnostic radiology, Yonsei University of medicine, Seoul, KR

Poster Nr 20

Objective :

- 1.to introduce the TNM staging standardized by American Joint Committee on Cancer (AJCC) and the International Union Against Cancer Committee (UICC)
- 2.to illustrate the T and N staging
- 3.to introduce the importance of preoperative staging

Materials and methods :

- 1.Review of TNM staging which was standardized by American Joint Committee on Cancer (AJCC) and the International Union Against Cancer Committee (UICC), 6th edition.
- 2.Practical application of T and N staging, using US, CT, MRI and PET.

Results :

Based on a series of illustrative cases with thyroid cancers, the advantages of US application at thyroid TNM staging over other modalities are shown.

Conclusion :

1. TNM staging of thyroid cancer is essential for radiologist to help the surgeon manage the patient preoperatively.
2. US plays an important role in diagnostic work-up.
3. Radiologists should be knowledgeable in imaging finding and its pitfalls.

CT characteristics of benign and malignant lesions of the jawbones

Y. Kim, B. Kim, H. Song

Department of Radiology, Uijongbu St.Mary's Hospital, Catholic University of Korea, Uijongbu, KR

Poster Nr 21

Objective :

To analyze the diagnostic role of CT scan in evaluation of benign and malignant lesions of the jawbones

Materials and methods :

We evaluated CT characteristics of many disease entities involving jawbones. Each one of the cases was pathologically proven.

Results :

Mandibular and maxillary lesions are odontogenic, nonodontogenic, odontogenic tumor-mimickers and tumor-like lesions. Role of CT was discussed in diagnosis of benign and malignant lesions of the jawbones.

Conclusion :

Careful consideration of the location of the lesion within the jawbones, its borders, its internal architecture, and its effect on adjacent structures generally makes it possible to narrow to the differential diagnosis.

A systematic approach of 3D-visualization of the ethmoid air cells and craniofacial sinuses based on clinical CT

C. Kober, I.B. Berg, S. Berg, R. Sader, H.F. Zeilhofer

HAW, Hamburg, DE

Poster Nr 22

Objective :

Segmentation, visualization, and 3D-reconstruction of the ethmoid air cells and the craniofacial sinuses from clinical CT-data in a reasonable amount of time

Materials and methods :

A special image processing algorithm applicable to clinical CT-data was developed. After application to CT-data, this contour filter provides thin black lines at tissue borders, especially the ethmoid air cells, the walls of the craniofacial sinuses, but also the orbital walls. This used for segmentation and subsequent 3D-reconstruction. As a variant, the filtered data set was subjected to direct volume rendering with a special, highly transparent transfer function.

Results :

The developed contour filter facilitates segmentation of the respective thin structures, namely the ethmoid air cells, the walls of the craniofacial sinuses, and also the orbital walls. The resulting 3D-models are characterized by high quality. The volume rendering of the filtered data set provides a very detailed view of the ethmoidal anatomy as well as of the sinuses which were not available so far.

Conclusion :

The presented new approach is of high technical efficiency with regard to the facilitated segmentation of the thin structures. Further, it is of high clinical significance for appropriate diagnosis support.

Can diffusion-weighted MR imaging differentiate benign from malignant tumors in the head and neck ?

R. Kohler, M. Viallon, X. Montet, M. Becker

Department of Radiology, Geneva University Hospital, Geneva, CH

Oral presentation

Objective :

The purpose of this prospective study is to evaluate the performance of diffusion-weighted MR imaging (DWI) in differentiating malignant from benign tumors in the head and neck.

Materials and methods :

One hundred nine lesions in 84 consecutive patients with clinical suspicion of tumor were examined prospectively by MRI at 1.5 T and 3 T. For all patients echo-planar imaging with thin slices (3 mm) in the axial plane was performed (with b values of 0 and 1000). The apparent diffusion coefficient (ADC) value was measured with a freehand ROI. Sixty-eight lesions were correlated with the pathologic diagnosis and 41 with clinical or imaging follow-up. Thirteen lesions were excluded because of the amount of artefacts precluding any reliable ADC measurement. In the 96 remaining lesions 19 were benign (11 benign salivary tumors, 3 cysts, 2 carotid space tumors, 1 lymphohemangioma, 1 lipoma, 1 angiofibroma), 40 were of inflammatory nature and 37 malignant (21 squamous cell carcinomas, 6 undifferentiated carcinoma, 5 adenocarcinoma, 3 malignant salivary gland tumors, 1 lymphoma, 1 esthesioneuroblastoma).

Results :

After an analysis of variance (ANOVA) with Bonferoni post-test correction, the mean ADC value was $2.22 + 0.87 \times 10^{-3} \text{ mm}^2/\text{s}$ for benign lesions, $1.26 + 0.52 \times 10^{-3} \text{ mm}^2/\text{s}$ for inflammatory lesions and $1.16 + 0.52 \times 10^{-3} \text{ mm}^2/\text{s}$ for malignant lesions. These results were statistically significant between the benign and malignant groups and between the benign and inflammatory groups ($p < 0.05$). All malignant tumors had an ADC value below $2.5 \times 10^{-3} \text{ mm}^2/\text{s}$.

Conclusion :

ADC values of malignancies appear to be lower than those of benign lesions but ADC of malignancies and inflammatory lesions are similar because of great scatter and overlap of data. If the ADC is above $2.5 \times 10^{-3} \text{ mm}^2/\text{s}$, a malignancy is very unlikely.

Contribution of MRI for detection of late complications of facial plastic surgery

R. Kohler, I. Masouye, M. Becker

Department of Radiology and Department of Dermatology, Geneva University Hospital, Geneva, CH

Poster Nr 23

Objective :

To evaluate the contribution of MRI in the detection of late complications of facial plastic surgery and injection of dermal fillers.

Materials and methods :

Eight female patients with erythema of the face and diffuse or localized swelling were investigated by MRI prior to biopsy. Clinically, a connective tissue disease or a vasculitis were suspected. The patients (mean age 52 years) had a history of facial plastic surgery, and were not aware of the type of material injected or implanted several years ago. The MR examinations were performed on a 1.5T or 3 T magnet using surface and/or phased-array coils, parallel imaging techniques and 3 mm thin, high-resolution slices (512 matrix for a field of view of 20 cm). The following sequences were obtained routinely: T1-weighted, T2-weighted, STIR, water saturated and fat saturated sequences, as well as T1- weighted images after injection of Gd-chelates.

Results :

Based on the MRI findings, the injected or implanted material was silicone (n=3), hyaluronic acide or collagen (n=4), goretex plate (n=1), autologous fat (n=1) and talc (n=3). The sequences with fat or water saturation and dedicated to silicone were of great help to characterize the composition of the injected or implanted substances. The areas of injection were easily detected by imaging and the diffuse inflammatory, granulomatous or fibrotic reactions and associated areas of fat necrosis were easily visible. The affected regions included the skin and subcutaneous fat, as well as the superficial musculoaponeurotic system (SMAS) of the face and the deeper facial muscles. MR imaging was used to select the most appropriate areas for surgical biopsy.

Conclusion :

MRI appears to be of great use in the diagnosis and characterization of inflammatory reactions to foreign bodies of the face especially when the clinical history is unclear. MRI is also useful in planning a biopsy or a surgical procedure.

Contribution of the CT and MRI angiography in the diagnosis of traumatic vascular injuries in the head and neck

R. Kohler, M.I. Vargas, K.O. Lövblad, J. Delavelle, P.A. Poletti, M. Becker

Department of Radiology, Geneva University Hospital, Geneva, CH

Poster Nr 24

Objective :

To illustrate the radiological aspects of open and closed vascular traumatic lesions in the head and neck by angio-CT and angio-IRM done in an emergency setting.

Materials and methods :

Retrospective review of the CT, MRI and clinical charts of 16 demonstrative cases of vascular injuries in the head and neck investigated by angio-CT and angio-IRM including 2D and 3D reconstructions in the emergency situation.

Results :

For each case we present the clinical context, the characteristic CT and / or MRI images with 2D and 3D reconstructions and the key diagnostic features. Open traumatic injuries (n =6) include unilateral vertebral dissection with false aneurysm caused by an edged foreign body, unilateral vertebral dissection with internal jugular vein injury following knife aggression, compressive hematoma of the neck following knife aggression, internal jugular vein occlusion caused by an abscess following intravenous drug injection, active bleeding secondary to a central venous catheter implantation and post-endarterectomy hematoma of the carotid sheath with vagal paralysis. Closed traumatic injuries (n=10) include uni- and bilateral carotid dissection, carotido-cavernous fistula, false aneurysm of the external carotid artery, uni- and bilateral vertebral dissection, false aneurysm of the vertebral artery, unilateral vertebral dissection with brachial plexus avulsion, unilateral vertebral dissection.

Conclusion :

In emergency situations angio-CT and angio-IRM allow a quicker and efficient triage of patients by diagnosing most traumatic vascular lesions and identifying associated bony and soft part lesions.

Cervical tuberculous adenitis: what are the most reliable ultrasound features ?

S. La'Porte, J.K. Juttla, H. Lloyd-Hughes, D. Remedios

Northwick Park Hospital, London, UK

Oral presentation

Objective :

The diagnosis of cervical TB adenitis is challenging and frequently overlooked. The purpose of this study is to identify the ultrasound features with the highest positive predictive value and specificity.

Materials and methods :

Our institution in West London is located close to a major international airport and has a catchment population which is diverse with a large proportion of minority ethnic groups and immigrants. We performed a retrospective review of ultrasound images and reports from 109 consecutive patients with suspected TB adenitis between 2002 and 2008. The diagnosis of TB was confirmed with either microbiology or cytology. Positive predictive values and specificities were calculated for nine particular ultrasound features: rounded shape, maximum diameter > 3cm, low echogenicity, level 4/5 involvement, unilateral presentation, peripheral flow pattern, presence of necrosis, matted nature and hilar preservation. In view of the high prevalence of disease in our study population, negative predictive values and sensitivities were not appropriate.

Results :

Of the 109 patients referred, there were 88 positive cases of TB adenitis (81%). Of the nine ultrasound criteria, the highest positive predictive values for diagnosing TB are: hilar preservation (86%), maximum diameter > 3cm (85%) peripheral blood flow (85%), matted nature (84%), presence of necrosis (84%), level 4/5 involvement (84%), low echogenicity (83%), round shape (81%) and unilateral presentation (80%). The most specific features are maximum diameter > 3cm (67%), hilar preservation (62%), peripheral flow (52%), matted nature (38%), level 4/5 involvement (38%), round shape (33%), presence of necrosis (33%), low echogenicity (24%) and unilateral presentation (19%).

Conclusion :

Of the 9 ultrasound criteria, those with the highest positive predictive value and specificity are hilar preservation, maximum diameter and peripheral blood flow. We advocate using these 3 features when assessing suspected cervical TB adenitis.

Neck TB or not TB: the value of ultrasound, cytology and microbiology for diagnosis

S. La'Porte, J.K. Juttla, H. Lloyd-Hughes, D. Remedios

Northwick Park Hospital, London, UK

Oral presentation

Objective :

The prevalence of TB is rising with cervical adenitis the second most common clinical presentation, but diagnosis is difficult without a gold standard. This study assesses the combination of ultrasound, cytology and microbiology to improve diagnosis.

Materials and methods :

Our institution in West London is located close to a major international airport and has a catchment population which is diverse with a large proportion of minority ethnic groups and immigrants. We performed a retrospective review of 109 consecutive patients with suspected TB adenitis between 2002 and 2008. Data were collected from computer-based ultrasound, cytology and microbiology reports and from individual departmental databases and hospital notes for missing results.

Results :

Of 109 patients with a high clinical suspicion of TB adenitis, 100 patients were considered on ultrasound to have TB as the first diagnosis but 5 of these had an alternative diagnosis confirmed on cytology. Ultrasound guided FNA was performed on all patients. On cytology, 81/109 (74%) were positive, 16/109 (15%) had an alternative diagnosis confirmed on cytology (reactive, metastases, lymphoma etc) and 12/109 (11%) were non diagnostic. On culture 67/109 (61%) were positive. Six out of 109 (6%) were smear positive, 2 of which were culture negative, but positive on cytology. Positive cytology and microbiology were obtained in 54 patients. Of the remainder, 21 (24%) patients had positive cytology alone and 13 (19%) were diagnosed on positive culture alone. Of those with a positive culture 54/67 (81%) were given an earlier cytological diagnosis. Combining cytology with microbiology, diagnosis was reached in 104/109 (95%) of patients with suspected TB, in whom 88 were proven TB.

Conclusion :

When TB is suspected US will suggest the diagnosis or an alternative and can guide FNA. Using combined cytology and microbiology diagnosis may be reached in 95% of cases. For immediate diagnosis cytology is really helpful but smear is rarely helpful.

Narrow duplicated or triplicated internal auditory canal: CT finding of three cases and review of the literature

S.Y. Lee, M.H. Jeon, I.H. Bae, G.S. Han, S.H. Cha, S.G. Kim, K.S. Park

Chungbuk National Univ. Hospital Gaesin-dong, Cheongju, KR

Poster Nr 25

Objective :

The narrow and duplicated IAC is very rare with only 5 cases in the literature and also there is no report about triplicated stenotic IAC in the literature. We present 2 cases of unilateral narrow duplicated IAC and 1 case of triplicated IAC.

Materials and methods :

3 children presented at our institute with abnormal findings on screening auditory function test at school and neonatal screening test. Audiological examination using pure tone audiometry revealed unilateral sensory neural hearing loss or profound hearing disturbance.

Results : HRCT revealed narrow and duplicated internal auditory canal in 2 patient (case 1&2) and another patient (case 3) were showed narrow and triplicated internal auditory canal at the same side with hearing disturbance. MRI was performed in one patient (case 3). 3D Fourier transformation- constructive interference in steady state (3D FT-CISS) images were showed the absence of vestibulocochlear nerve (CN VIII) at Rt. CPA cistern. Superior canal contained nerve structure though to be facial nerve, but no nerve was identified in middle and inferior canals.

Conclusion :

This report supports to the association between a narrow IAC and aplasia or hypoplasia of the vestibulocochlear nerve. The separated, accessory bony canals delineated on HRCT never mean the presence of nerve fiber.

Evaluating thyroid nodules: can ultrasound accurately predict and select neoplastic nodules for fine needle aspiration (FNA) cytology

R.K. Lingam, S. Kaneira, M. Qarib

Dept of Radiology, Northwest London Hospitals, London, UK

Oral presentation

Objective :

To assess diagnostic performance of ultrasound in detecting neoplastic thyroid nodules and thereby selecting nodules for fine needle aspiration cytology.

Materials and methods :

Eighty-nine patients that were referred for thyroid ultrasound examination with thyroid nodule(s) were prospectively and independently assessed by two experienced observers (radiologist and sonographer) with regards to nodular characteristics (echogenicity, calcification, contour and doppler vascular flow pattern) in an attempt to detect neoplastic nodules and hence select nodules for Fine Needle Aspiration (FNA) Cytology. Nodules were classified as neoplastic (benign and malignant tumours) or non-neoplastic on a 5-point confidence level scale as follows: 1) Definitely non-neoplastic, 2) probably non-neoplastic, 3) possibly neoplastic requiring FNA, 4) probably neoplastic requiring FNA and 5) definitely neoplastic requiring FNA. Sonographic prediction was compared to cytological diagnosis to assess whether sonography can reliably predict thyroid neoplasia and thereby select nodules for FNA cytology.

Results :

FNA cytology diagnoses included 16 (18.0%) neoplastic nodules and 70 (78.7%) non-neoplastic nodules. 3 patients with non-diagnostic FNA results were excluded. In detecting neoplasia (confidence level scores 3-5), a sensitivity and NPV of 100% was achieved, with a specificity of 81% and PPV of 55%. 57/70 non-neoplastic nodules (79%) were correctly diagnosed thereby obviating the need for FNA cytology. The low specificity and PPV was a result of 13 non-neoplastic nodules, all with confidence level scores of 3. Of the neoplastic nodules, 3/16 nodules had confidence level scores of 3. There was very good interobserver agreement ($k > 0.9$).

Conclusion :

In our series, a high NPV with very good inter-observer agreement suggests that ultrasound assessment has a role in accurately and reproducibly predicting non-neoplastic nodules, and therefore in selecting nodules that do not require FNA. Eventhough we could not accurately predict neoplasia, all neoplastic nodules were selected for FNA cytology analysis.

Multidetector CT (MDCT) in the diagnosis of sinonasal osteoma

A. Lo Casto, F. Ganguzza, P. Collodoro, G. Cavarretta, A. Comparetto, G. La Tona

Dipartimento di Biotecnologie mediche e Medicina legale Università degli Studi di Palermo and Fondazione Istituto San Raffaele G. Giglio Cefalù, Palermo, IT

Oral presentation

Objective :

Sinonasal osteoma (SO) is a benign bone forming tumor, usually asymptomatic and an incidental finding during maxillofacial imaging. The aim of this paper was to make a retrospective analysis on 229 patients studied by MDCT for sinusitis.

Materials and methods :

The MDCT (40-64 rows) studies, performed between 2005 and 2007, of 229 consecutive patients (124 men, 105 women), were retrospectively analyzed. SO were classified according to site, size and eventual symptoms.

Results :

SO were observed in 11/229 patients (8 men, 3 women, age range 17-81 years, 4,8% incidence). In these 11 patients the SO site was: the frontal sinus in 6/11 (55%), 3/11 (27%) the ethmoid cells, 1/11 (9%) the sphenoid sinus, 1/11 (9%) the right middle turbinate. The diameter of SO ranged between 3 mm and 4.7 cm. In 6/11 patients sinusitis of the affected sinus was observed. In 2/6 patients the SO narrowed the nasofrontal duct. In 1/11 patients the SO originated in the frontal sinus and extended towards the orbit and ethmoid cells.

Conclusion :

MDCT allows to detect SO, to evaluate its extension, to define its relationships with adjacent and thin bony structures of the ostiomeatal complex and with the orbital cavity, to detect associated sinusitis.

Langerhans cell histiocytosis (LCH) of the jaws. Panoramic radiography, CT and MRI findings

A. Lo Casto, F. Coppolino, F. Ganguzza, S. Salerno, R.T. Bruno, G. La Tona

Dipartimento di Biotecnologie mediche e Medicina legale Università degli Studi di Palermo and Fondazione Istituto San Raffaele G. Giglio Cefalù, Palermo, IT

Poster Nr 26

Objective :

LCH is a rare disease with a reported incidence of 3 cases/million population. LCH of the jaws accounts for 6% of all lesions. 3 cases studied by panoramic radiography, CT and MRI are described.

Materials and methods :

3 women (age range 6-77 years) affected by LCH of the jaws were studied by panoramic radiography, CT with MPR and dental reformatting software, and MRI with and without i.v. paramagnetic contrast medium.

Results :

On panoramic radiography a unilocular radiolucent lesion with poorly defined borders and floating teeth was appreciable. On CT the lesion was hypodense, causing enlargement of the involved bone segment, thinning and interruption of cortical bone, and periosteal reaction. In 1 patient the mandibular canal was involved. On MRI the lesion was hypointense on T1, inhomogenous on T2, slightly enhancing after i.v. paramagnetic contrast medium. Contiguous soft tissue swelling was associated. In all patients a mixed lesion was recognized at histology.

Conclusion :

LCH of the jaws is first recognized on panoramic or conventional radiographs. CT allows a better evaluation for bone cortical destruction, mandibular canal, maxillary sinus and nasal cavity involvement. MRI is useful for soft tissue evaluation.

Tongue hemiatrophy: a silent sign for skull base pathology

L. Lopes, D. Coutinho

Hospital de Santa Maria, Lisbon, PT

Poster Nr 27

Objective :

Hypoglossal nerve palsy may be clinically silent though obvious on imaging. Bone CT determines skull base changes. MRI gives the lesion matrix, origin and extension. The association of both narrows the differential diagnosis, pointing to a final diagnosis

Materials and methods :

The authors report two cases of unilateral hypoglossal nerve palsy. In case 1 the cause of the palsy appeared to be a jugular foramen schwannoma with extension within the hypoglossal canal. In case 2 the patient complained about pulsatile tinnitus. An expansible mass with permeative-destructive pattern on bone CT and multiple black dots on MRI revealed a glomus jugulare paraganglioma.

Results :

The hypoglossal nerve controls the movements and shape of the tongue. The fibers emerge on the surface of the medulla oblongata between the pyramid and the olive. They then cross the posterior cranial fossa and leave the skull through the hypoglossal canal. Lesions of the hypoglossal nerve may occur anywhere along its course and may result from tumor, demyelinating disease, syringomyelia, vascular accidents among others. In our study, neither patient complained of any disability. On observation the tongue deviated toward the healthy side at rest and toward the affected side on protrusion. With bone CT obvious skull changes were seen. On MRI hemiatrophy of the tongue with fatty displacement was best demonstrated by means of T1-weighted magnetic resonance imaging. Skull base lesions that affect the hypoglossal nerve may present with tongue hemiatrophy.

Conclusion :

Although clinically silent, tongue hemiatrophy may be an indirect and silent sign for skull base pathology. The imaging combination of bone CT and T1W MRI may be the best way to shorten the differential diagnosis and reach a final aetiology.

PET-CT pitfalls in head and neck pathologies

K. Masterson, R. Kohler, O. Ratib, C. Steiner, M. Becker

Department of Radiology, Geneva University Hospital, Geneva, CH

Poster Nr 28

Objective :

To illustrate the most common interpretation pitfalls in the head and neck area linked to physiological FDG uptake in patients imaged with PET-CT.

Materials and methods :

Our study is based on the retrospective analysis of 117 consecutive PET-CT studies performed in 97 patients with known or suspected head and neck tumors during the past 2 years. The PET-CT protocol included whole body low dose unenhanced CT used for attenuation correction, followed by a thin-sliced contrast enhanced CT 60 minutes after injection of 250-380 MBq FDG.

Results :

False positive interpretations of PET-CT findings were caused by an unusual FDG uptake in 15 patients in whom additional imaging studies, as well as percutaneous or endoscopic biopsies were performed in order to solve the diagnostic dilemma. Pitfalls causing diagnostic problems included: major asymmetric physiologic uptake of the upper Waldeyer ring or tongue base, which were interpreted as possible tumors; asymmetric physiologic or focal uptake of the thyroid gland caused by benign nodules; physiologic accumulation of FDG in several muscles, such as the intrinsic tongue muscles, the vocal cords, the thyrocricoid muscle, the sternocleidomastoid muscle and the pterygoid muscles and inflammatory tissue and scars following surgical resection or radiation therapy. Asymmetric physiologic muscle uptake was often seen in patients with unilateral paralysis or unilateral resection and compensatory contraction of contralateral muscle groups. False negative PET-CT interpretations occurred in 2 patients and were caused by small tumors with low FDG avidity.

Conclusion :

Misinterpretation of PET-CT images can be avoided by being aware of possible pitfalls in PET-CT image interpretation, in particular physiologic FDG uptake linked to normal lymphatic tissue and asymmetric contracting muscles after surgery and radiation therapy.

Tumors and tumor-like lesions of the orbit: radiologic-pathologic correlation

K. Masterson, R. Kohler, M.I. Vargas, J. Delavelle, M. Bongiovanni, M. Becker

Department of Radiology and Department of Pathology, Geneva University Hospital, Geneva, CH

Poster Nr 29

Objective :

The aim of this scientific exhibit is to illustrate the imaging, clinical and histopathologic features of the most common orbital tumors and tumor-like lesions in children and adults.

Materials and methods :

Retrospective review of 64 cases of orbital tumors and tumor-like conditions seen during a period of 3 years at our institution. CT and/or MRI were available for review in each patient. All CT examinations had been performed using 1 mm thin slices obtained after iv injection of iodinated contrast material. The MRI examinations had been done using 0.7-3 mm thin slices and a combination of head and surface coils. The sequences performed included FSE T2, FSE T1 ± fat saturation and ± iv gadolinium-chelates, 3D GRE and VIBE.

Results :

After a basic review of orbital anatomy, we present the most frequent orbital tumors and tumor-like conditions in a systematic fashion. In our series of 64 patients, we had, 49 benign lesions and 15 malignant tumors. Benign lesions included: meningioma (n=10), inflammatory pseudo-tumors (n=9), hemangiomas (n=6), tumors of the lacrymal apparatus (n=6, including mucoceles, pleomorphic adenomas, lacrymal gland cysts, lacrymal sac hemangioma), dermoids (n=4), sino-nasal mucoceles (n=4), lymphangiomas (n=2), neurofibromas (n=2), hematomas (n=2), lipoma (n=1), myofibroblastoma (n=1), corneal papilloma (n=1) and fibrous dysplasia (n=1). Malignant tumors included primary orbital lesions (n=10, lymphoma and leukemia, spinocellular carcinoma, squamous cell carcinoma, basocellular carcinoma, sebaceous carcinoma, rhabdomyosarcoma) or metastases to the orbit (n=5 including breast and lung carcinomas, melanoma, liposarcoma).

Conclusion :

A variety of benign and malignant tumors may arise in the orbit. They may originate either in the orbit itself, in adjacent structures like sinuses or skin or in distant sites. In addition, pseudo-tumoral conditions may mimic true neoplasms. Knowledge of these entities and of their characteristic imaging features are essential for tumor characterization, precise depiction of the tumor spread and for planning of biopsy or surgery.

Intra-arterial infusion chemotherapy for head and neck SCCs with mandibular invasion

T. Nakasato, M. Hitachi, H. Oikawa, R. Nakamura, S. Ehara, M. Izumisawa

Iwate Medical University, School of Medicine and Dentistry, Morioka, JP

Poster Nr 30

Objective :

Head and neck SCCs (NHSCCs) with destruction of the mandible are usually difficult to obtain complete response to chemoradiotherapy. Therefore, surgical treatment is the first choice in such cases. Recently, advanced superselective intra-arterial infusion chemotherapy for HNSCCs accomplishes high control rate with preserving organic function and cosmetic, and it helps maintain high quality of life. We evaluated treatment response and bone formation to combined radiation and intra-arterial infusion of docetaxel(DOC) or DOC plus CDDP for HNSCCs with mandibular invasion.

Materials and methods :

Eleven patients (6 men, 5 women, ave.age of 73) were evaluated with two protocols of intra-arterial infusion as monthly (Docetaxel ,DOC, 40mg/?2) or weekly regimen (DOC, 15mg/m2 plus CDDP, 50mg/body). The patients had carcinoma of lower gingiva (n=8), oropharynx (1), floor of the mouth (1), lower lip (1); and the staging was stage II (n=1), and IV (10), respectively. Superselective catheterization was performed by the standard femoral artery approach under local anesthesia. The coaxial system of 5-Fr guiding catheter, and 2.1 Fr. microcatheter were used under the systemic heparinization. Facial, lingual, inferior alveolar arteries were selected for infusion of anti-tumor agents to the primary tumor and muscular branches of occipital artery to metastatic lymph nodes. Concurrent radiotherapy of 40-60Gy was performed for all the patients. To detect bone remodeling, dental MPR was performed in all the patients.

Results :

Complete (CR) and partial responses (PR) were observed in 9 (4 of pCR) (82%) and 2 patients (18%), respectively. Salvage surgery was performed in the two patients. 3-year survival rate was as high as 87.5%. Bone remodeling was observed in 63.6%. The case shown bone remodelling were all CR, finally.

Conclusion :

Superselective intra-arterial infusion chemotherapy as a part of TPF protocol including concurrent radiotherapy has a potentially high control rate and we may be able to expect bone regeneration even with mandibular invasion. Aggressive mandibulectomy may also be avoided after the treatment. For this purpose, dental MPR is a useful diagnostic tool for detecting subtle bone formation.

The face predicts the brain: the association of facial malformations and brain anomalies in fetuses with trisomy 13 in fetal MRI

S.F. Nemeč, P.C. Brugger, C. Czerny, D. Prayer

Department of Radiology/Division of Neuroradiology and Musculoskeletal Radiology and Center of Anatomy and Cell Biology, Integrative Morphology Group, Medical University Vienna, Vienna, AT

Oral presentation

Objective :

Since the 1960s, the literature describes that congenital facial anomalies can predict brain anomaly. Therefore, findings in facial malformations in fetuses with trisomy 13 were reviewed in advanced fetal MR imaging which allows to visualize the viscerocranium and correlated with potential brain anomalies.

Material und methods :

This retrospective study included six fetuses (16-34 gestational weeks, mean 28) with facial malformations, depicted in fetal MRI. MRI was performed on a 1.5 Tesla unit using a five-element phased-array surface coil. In addition to a standard MRI protocol [T1- and T2-weighted (w) sequences, diffusion weighted imaging (DWI)] the following dedicated sequences were used to image the viscerocranium: axial, coronal and sagittal T2-w sequences, a 3D thick-slab T2-w sequence, and a coronal single shot fast field echo (SSh FFE) sequence (=echoplanar imaging/EPI). The evaluation focused on facial structures and on the presence of facial clefts as well as on brain structures.

Results :

Midface malformations, which consisted of hypotelorism (4), arhinia (3), median facial cleft (1) and lip-palate-jaw clefts (3) were associated with holoprosencephaly (alobar or semilobar) in four fetuses, with pachygyria in four fetuses, with missing olfactory nerve in four fetuses, with a frontoethmoidal meningoencephalocele in one fetus and with a liquor space anomaly in one fetus, respectively. Additional facial malformations comprised dolichocephaly (2), microcephaly (2), micrognathia(2) and microtia (1).

Conclusion :

Fetal MRI allows a precise visualization of facial malformations which are frequently related with brain anomalies. Specific patterns of facial malformations might be early signs of typical brain anomalies in fetuses with trisomy 13.

Cranial neuropathies as a manifestation of systemic disease

T. Palma, I. Cravo, C. Gonçalves, A. Germano, S. Costa, A. Valverde

Neuroradiology Division, Hospital Fernando Fonseca, Lisbon, PT

Poster Nr 31

Objective :

Cranial neuropathies are infrequent manifestation of systemic disease. The most common etiologies involved are inflammatory/granulomatosis, infection, autoimmune and neoplastic diseases as well toxic insults. A retrospective study using MRI data acquired between January 2005 and May 2008 was performed including abnormal brain examinations of patients with isolated or multiple cranial neuropathies as initial manifestation of a systemic disease.

Materials and methods :

Eleven patients were studied with a MRI protocol that includes fluid attenuated inversion recovery (FLAIR) weighted images, diffusion-weighted imaging (DWI) and T1 weighted imaging pre and post-gadolinium contrast injection.

Results :

All the patients had abnormal brain MR findings characterized mainly with enhancement of cranial nerves on the post-contrast T1 WI. Three patients had non Hodgkin disease and another three had Lyme disease; three patients had infection disorders and two patients had meningeal carcinomatosis.

Conclusion :

T1 weighted imaging post-gadolinium contrast studies are essential to establish MRI diagnosis of cranial neuropathies in the clinical setting of systemic diseases.

Interobserver agreement at the malignant thyroid nodules with conventional ultrasound (US) and US elastography: prospective study

S.H. Park, J.Y. Kwak, S.J. Kim, M.J. Kim, E.K. Kin

Gachon University Gil Medical Center, Diagnostic Radiology, Breast Division, Guwol-dong, KR

Oral presentation

Objective :

to investigate interobserver agreement at the malignant thyroid nodules with conventional B-mode US and real-time free hand US elastography

Materials and methods :

From 2007.12. to 2008.2, 42 patients (age range, 19-73 years; mean age, 45.0 ± 12.2 years) with 52 thyroid nodules were examined with conventional B-mode US and real-time free hand US elastography. All the patients were scheduled to undergo thyroid surgery due to thyroid nodule proven to be malignant on aspiration cytology. Three radiologists independently performed conventional US and elastography and analyzed US images. Analysis in conventional US included composition, nodular echogenicity, margin, calcification, shape, underlying parenchymal echogenicity and final assessment. Ueno classification and odds ratio were made by using US elastography. Interobserver agreement was evaluated with Spearman correlation analysis except the area ratio (Pearson correlation analysis). $P < .05$ was considered to indicate significance.

Results :

Statistically significant ($p < .05$) concordance between 3 radiologists was found for most US features except for nodular echogenicity and margin of thyroid nodules on conventional US. The highest value of concordance was achieved in composition (Spearman correlation coefficient; 0.70-1.00), followed by underlying parenchymal echogenicity (0.52-0.83), shape (0.48-0.79), calcification (0.47-0.62) and final assessment (0.29-0.50). The least concordant finding was margin (-0.09-0.54) and nodular echogenicity (0.04-0.45) on conventional US. However, there was no statistically significant concordance in Ueno classification (Spearman correlation coefficient; 0.08-0.22, $p > 0.05$) and area ratio (-0.03-0.23, $p > 0.05$) on elastography.

Conclusion :

Conventional US made statistically significant concordance between radiologists in most of US features, however, US elastography did not make reliable interobserver agreement at malignant thyroid nodule.

Comparison of low-dose with standard-dose and an optimized FESS-protocol in multidetector CT examinations of paranasal sinuses

F. Pekiner, K. Orhan, P. Berglund, L.T Flygare

Department of Oral Diagnosis & Radiology, School of Dentistry, Marmara and Ankara University, Department of Oto-Rhino-Laryngology and Department of Radiology, Sunderby Hospital, SE

Poster Nr 32

Objective :

To compare the diagnostic image quality between a low-dose protocol, a standard-FESS and an optimized FESS-protocol and to evaluate the possible use of a low-dose multidetector CT (MDCT) protocol for preoperative sinus examination.

Materials and methods :

50 low dose MDCT paranasal sinus examinations, 50 standard-FESS and 50 optimized FESS protocol examinations were retrospectively picked from the PACS. The groups were matched with respect to spectrum and frequency of pathological findings, age and gender. Three dentomaxillofacial radiologists and one ENT-surgeon evaluated the images. Before the evaluation all observers were calibrated and reference images were available during the readings. Examination protocol as well as information on the patient was blinded to the observers. The visualisation of anatomic landmarks important in FES-surgery was judged as well as the periodontal space of upper molars. The contrast of eye muscles vs. orbital fat, presence of pathology and whether diagnostically relevant structures were obscured by artifacts caused by metal fillings was noted. Overall subjective diagnostic quality of the images was also estimated. The observations were graded according to a 3-point confidence scale.

Results :

Kappa analysis indicated a strong intra-observer agreement ($r=0.95$). Inter-observer agreement for the detection of anatomic landmarks ranged between low to substantial (Kappa= 0.460-0.850). Agreement where higher between the three most experienced readers Kappa-values ranging from 0.62-0.85. Agreement between readers were lower in the presence of pathology. Although image noise was higher in the low-dose portocol, Chi-square analysis detected no significant difference in subjective image quality score among the 3 imaging protocol groups ($p>0,05$). Image quality was heavily dependant on pathology scoring (P

Conclusion :

Low-dose MDCT ($\sim 0.1\text{mSv}$) gives a substantial dose reduction compared with standard-dose protocols but without clinically relevant difference in subjective image quality or detection of the most important anatomic landmarks for preoperative evaluation.

Image fusion between echo-planar diffusion-weighted (EP-DW) and isotropic 3D VIBE post-Gd in head and neck: a feasibility study.

M. Ravanelli, D. Farina, E. Botturi, A. Borghesi, R. Maroldi

Spedali Civili, Università degli Studi di Brescia, Brescia, IT

Oral presentation

Objective :

The fusion of EP-DWI and isotropic 3D VIBE post-Gd sequences may combine the strengths of both functional and volumetric imaging, overcoming low-spatial resolution affecting EP-DWI. Feasibility and accuracy of this technique are the aim of the study.

Materials and methods :

Twenty consecutive patients underwent a MR study for a primary neoplasm of head and neck. Six studies were focused on the neck region, 7 on the oral cavity and 7 on the paranasal sinuses. MR protocol comprised both EP-DWI sequences and post-gadolinium 3D VIBE sequences. The parameters of EP-DW sequences were the following: TR/TE 5000/83 ms, matrix 128x128, FOV 250 mm, phase encoding direction A-P, slice thickness 4 mm, SPAIR, NEX 4, b₀/1000, 1?35?. Fusion matching was first performed between b₀ and 3D VIBE images; co-registration parameters were then applied to b₁₀₀₀ images; a further tuning was finally performed between b₁₀₀₀ and VIBE images, using as landmarks the hyperintense structures on b₁₀₀₀ images, except tumor. Mismatch between the center of these structures on b₁₀₀₀ and 3D VIBE images was measured in all three major axes using ?side by side? visualization modality.

Results :

Matching between b₁₀₀₀ and 3D VIBE images was performed on 161 anatomical structures (8.5 structures/examination). Mean mismatch on antero-posterior direction (phase encoding direction) was 1,82 mm (0-8 mm; 95% interval of confidence 0,21 mm); on transversal direction was (0-2.5 mm; 95% interval of confidence 0.74 mm); on cranio-caudal direction was 0,85 mm (0-3 mm; 95% interval of confidence 0.08 mm). No statistical difference was obtained among the studies focused on neck, oral cavity and paranasal sinuses.

Conclusion :

The mismatch between b₁₀₀₀ and VIBE images was larger in the phase encoding direction. Although EP-DW sequences are affected by spatial distortion and susceptibility artifacts, fusion between EP-DWI and 3D VIBE images is feasible and accurate.

Optimization of echo-planar diffusion-weighted (EP-DWI) sequences in the head and neck: signal/noise ratio and ghosting artifacts

M. Ravanelli, D. Farina, E. Botturi, A. Borghesi, R. Maroldi

Spedali Civili, Università degli Studi di Brescia, Brescia, IT

Oral presentation

Objective :

Susceptibility artifacts and insufficient signal/noise ratio (SNR) on b1000 images are the main drawbacks of EP-DWI in head and neck. Therefore, the optimization of sequence parameters represents an imaging hot topic and is the aim of the study.

Materials and methods :

Three EP-DW sequences with different parameters were tested on head and neck region of five volunteers: 1. TR/TE 3200/80 ms, 128x128, NEX 7, slice thickness 4 mm, fat-sat, b0/1000, 1?39?; 2. TR/TE 5000/80 ms, 128x128, NEX 4, slice thickness 4 mm, SPAIR, b0/1000, 1?35?; 3. TR/TE 3200/80 ms, NEX 4, slice thickness 4 mm, fat-sat, b0/1000, 1?01?. In all three sequences, a manual magnetic field adjusting was performed before the acquisition start. SNR was calculated for each sequence at the thyroid gland and oral floor levels. Ghosting artifacts were visually assessed and measured by a dedicated home-made software. ANOVA test for dependent populations was used to compare SNR values obtained with the three different sequences.

Results :

Sequence 1 showed an higher SNR at the thyroid level (+30% vs sequence 2, +17% vs sequence 3; p 0,049). Ghosting artifacts value was higher in sequence 1, in relation to the higher SNR, although their spatial distribution, visually evaluated, was nearly the same in all three sequences.

Conclusion :

In the neck, an adequate SNR can be achieved by increasing NEX; SPAIR reduces SNR in this region. Minimization of artifacts is a priority: the method for the quantitative assessment of artifacts is too SNR-dependent and needs further developments.

MR Imaging of a human nasopharynx tumor on a cellular level using iron oxide nanoparticles of different sizes

O. Saborowski, F. Santini, M. Fani, K. Mueller, P. Robert, J.M. Froehlich, G. Bongartz

Medical Radiology, Radiological Physics and Radiological Chemistry, University Hospital Basel, and Research, Guerbet Group, Aulnay-Sous-Bois, FR, Basel, CH

Poster Nr 33

Objective :

To image human KB tumor cells using iron oxide nanoparticles. Two iron oxides with superparamagnetic properties of different sizes were compared: ferumoxtran-10 (Sinerem®, Guerbet, France) and ferumoxides (Endorem®, Guerbet, France).

Materials and methods :

10 Mio human KB nasopharynx carcinoma cells were labeled with increasing doses at 8.5, 17, 34 and 68 µg Fe/ml of ferumoxtran-10 and at 4.25, 8.5, 17 and 34 µg Fe/ml of ferumoxides for 24 hrs at 37°C. Additionally 3.0- 0.05 x 10 Mio KB cells were labeled with ferumoxides at a dose of 68 µg Fe/ml and ferumoxtran-10 at a dose of 136µg Fe/ml) for 4 and 12 hrs. After the uptake all cells were imaged in 0.5 ml isotonic Ficoll solution prepared in test vials at clinical 1.5T and 3T MR scanners. Cells were dissolved in Ficoll and not centrifuged down, in order to allow quantitative R1/R2 assessments. Images were obtained with a sag 2D spin echo sequence (multiple TR values of 100-2000 ms, TE = 11 ms, FOV = 0.47x0.47x5 mm³, matrix = 256x104, slice thickness = 5 mm and a multi-contrast 2D spin echo sequence (same resolution, TR = 4000ms and 32 contrast with echo spacing of 18ms). For comparison, iron oxide concentrations within the cell samples were measured by ICP-MS.

Results :

Measurements of R1 and R2 were feasible in all samples with dose-dependent increase of iron labelling and cell density. Best labelling results were achieved with SPIO after 12 h incubation at 68 µg Fe/ml. Acceptable R2 relaxations rates for ferumoxides and ferumoxtran-10 of the samples could be measured with different contrast agent doses at 1.5 T and 3 T. Best labelling results could be achieved with Endorem-labeled KB cells at decreasing cell numbers after 12 hrs incubation with a concentration of 68 µg Fe/ml. Ferumoxides labelled cells showed an higher iron uptake than ferumoxtran-10 labelled cells determined by ICP-MS.

Conclusion :

MR imaging shows the homogenous distribution of human KB nasopharynx carcinoma cells within Ficoll solution at clinical 1.5T and 3T. Visualization of KB tumor cells is feasible using superparamagnetic iron oxide nanoparticles of different sizes.

Comparable evaluation of radiological methods in dental implantology based on evidential medicine principles

N.S. Serova., A.Y. Vasiliev, A.I. Ushakov, I.N. Gipp

Moscow State University of Medicine and Dentistry, Moscow, RU

Poster Nr 34

Objective :

To perform the comparable analysis of diagnostic radiological methods efficiency in dental implantology subject to evidential medicine principles.

Materials and methods :

50 patients were examined (20 female and 30 male) with an age from 19 to 54, prior and post stomatological implantation operations. At the planning stage all patients had undergone orthopantomography. 24 patients had undergone spiral CT with dedicated dental programs; 26 had undergone cone beam dental tomography.

Results :

Spiral CT and cone beam dental tomography had allowed more accurate determination of bone condition; distance to mandibular canal measurement; finding of concomitant pathology (like inflammation changes in sinuses, foreign bodies). The sensitivity of orthopantomography was 84.3%, spiral CT ? 95.6%, dental cone beam CT ? 96.0%; specificity was 72.6%, 91.5%, 92.9%; precision was 79.4%, 93.1%, 94.5% correspondingly. Orthopantomography had allowed better surrounding implantation area condition determination including periimplantitis at the postoperative stage, which was difficult with CT and cone beam dental CT due to artifacts problem. But computed were more effective in complication evaluation (like maxillary sinuses walls perforations and sinusitis; mandibular canal injuries). The sensitivity of orthopantomography was 72.3%, spiral CT ? 97.6%, dental cone beam CT ? 98.2%; specificity was 71.0%, 93.8%, 90.2%; precision was 71.5%, 95.2%, 91.3% correspondingly.

Conclusion :

Evaluation of the radiology method based on evidential medicine principles allows effective stomatological implantation.

CT and MR evaluation of proptosis

H.H. Song, Y.J. Kim, B.S. Kim

Cheju Halla Hospital, Jeju, KR

Poster Nr 35

Objective :

To analyze the diagnostic role of CT and/or MR imaging in the evaluation of proptosis.

Materials and methods :

We evaluated CT and/or MR images of various disease entities presenting with proptosis. All cases were confirmed pathologically or clinically.

Results :

We categorized various disease entities causing proptosis into 1) congenital & developmental 2) infection & inflammatory 3) trauma 4) vascular 5) neoplastic , and 6) miscellaneous lesions. Role of CT and/or MR was evaluated in defining the cause of proptosis and the nature and extent of the lesions causing proptosis.

Conclusion :

This exhibit illustrates various disease entities causing proptosis.

Neck phlegmon with fistula-case report

T. Stavric, N. Sekularac, I. Jovanovic-Stavric

Department of radiology, KBC Dragisa Misovic, Belgrade, CS

Poster Nr 36

Objective :

The aim of this case study was to present importance of urgent neck ct examination with contrast media in order to diagnose and evaluate extension of deep neck infections.

Materials and methods :

Patient,78 years old female hemodialysed for past 25 years with dissecant aneurism of left common carotid artery and reccurent pharyngeal infections and concomitant regional lymphadenopathy was clinically presented with fever,torticollis, odynophagia and leaking of purulent content from opening on infralaryngeal region.After clinical investigation patient sent to radiology department for ct examination of neck.Neck ct was performed on 16 slice MSCT using neck routine protocol on 3 mm slice first without contrast than after intravenous administration of 100 ml contrast media with MPR on 0.6 mm.

Results :

Axial neck ct shows large not clearly bordered necrotic area with gas in left parapharyngeal space which extend into the submandibular space and laterally involving the carotid sheath with spreading of infection into the thrombotic dissection of left common carotid artery. This mass also narrows the lumen of pharynx with fistula that exceeds infralaryngeal region. These findings suggest diagnosis of neck phlegmon and patient was immediately surgically treated because of this life threatening condition.

Conclusion :

Our study implicates the importance of urgent neck ct examination when deep neck infection is suspected especially in elderly patients with diab.mellitus, immunocompromited or,as in this case, hemodialysed patients with reccurent pharyngeal infections.

"Diseased mastoid air cell" due to epineurial pseudocyst of the intratemporal facial nerve

S.C.A. Steens, B. De Foer, R. Hermans, B.M. Verbist

Dept. of Radiology and Leiden University Medical Center, Leiden, NL, Sint-Augustinus Hospital, Antwerp, BE and UZ Leuven, Leuven, BE

Poster Nr 37

Objective :

The epineurial pseudocyst of the intratemporal facial nerve is an uncommon entity mimicking mastoid air cell disease. To increase the familiarity with this entity amongst referring physicians and radiologists, we report CT and MR findings in 8 cases.

Materials and methods :

Eight patients with imaging findings compatible with epineurial pseudocyst of the intratemporal facial nerve (nVII) as first described by Pertzborn et al. in *Otology and Neurotology* in 2003 (24:490-493) were collected at three hospitals. Patient demographics, clinical presentation, clinical findings and imaging features on CT (n=8) and MR, including diffusion weighted imaging (DWI) (n=2), were retrospectively reviewed.

Results :

All patients (6f, 1m, mean age 30y, range 5-54y) presented with symptoms and signs unrelated to nVII. CT showed a sharply demarcated, round to oval structure with soft tissue density posterior to and abutting the mastoid portion of the nVII canal, mimicking the appearance of an opacified mastoid air cell. On T2-weighted sequences a sharply delineated hyperintense lesion was found in the signal void of the temporal bone. On T1-weighted sequences, the lesions appeared hypointense. Non-EPI DWI (B1000) showed no hyperintensity, excluding the diagnosis of a congenital cholesteatoma. Since none of the patients had symptoms attributable to the intratemporal nVII, these findings can be considered coincidental and probably of no clinical significance. However, when CT of the temporal bone is performed in a preoperative evaluation, the presence and recognition of this lesion may have implications for surgical approaches such as in placement of a cochlear implant or mastoidectomy.

Conclusion :

An nVII epineurial pseudocyst is an uncommon finding, probably without clinical significance. Knowledge of the imaging appearance will prevent unnecessary follow-up examinations in asymptomatic patients. Its presence may be important to surgeons.

MR imaging of the larynx - the way forward ?

N.J. Stephens, S. Punwani, T. Beale, S. Morley

University College London Hospital, London, UK

Oral presentation

Objective :

To show the efficacy of a motion correction MR sequence for imaging the larynx.

Materials and methods :

High resolution axial and coronal T2-weighted images of the larynx were obtained in one healthy subject using standard acquisition techniques and Siemens syngo® BLADE sequences. Multiple sequences were acquired in a randomised fashion, the subject coughing and swallowing at specified intervals throughout image acquisition. Images assessed for diagnostic value independently by two specialist consultant radiologists using predetermined criteria.

Results :

Both radiologists found the images acquired using the motion correction sequence of superior diagnostic quality to those acquired using standard k-space sampling techniques.

Conclusion :

The use of a motion correction sequence (Siemens syngo® BLADE) provides good quality, diagnostic high resolution images of the larynx despite patient movement throughout image acquisition. The images are superior to those acquired using standard acquisition techniques. We advocate the use of this sequence in imaging the larynx and postulate its role in the staging of laryngeal carcinoma.

Imaging assesment of lymph nodes

N.J. Stephens, S. Brown, E.J. Adam

St Georges Hospital, London, UK

Poster Nr 38

Objective :

To assess the effect a change in the current criteria for lymph node disease would have on accuracy of identifying metastatic nodal disease in the neck

Materials and methods :

All neck dissection specimens from January 2006 - December 2006 had their pre-operative images reviewed retrospectively to ascertain number of pathologically enlarged lymph nodes using criteria of >1cm short axis dimension. Reassessment performed using new criteria of >1cm long axis dimension. Correlation with malignant nodes in the dissection specimens to assess impact the change in size criteria would have on sensivity and specificity

Results :

83 patients had neck dissections and cross-sectional imaging available. 29 patients had metastatic lymph nodes. Using the new criteria resulted in an increase in the positive predictive value but with a significant increase in the number of false positives.

Conclusion :

Identifying metastatic nodal disease in patients with head and neck cancer remains controversial. We assessed the effect a change in the current widely accepted criteria of >1cm short axis to >1cm long axis would have on this group of patients.

Laryngeal ultrasound

N.J. Stephens, S. Morley, T. Beale

University College London Hospital, London, UK

Poster Nr 39

Objective :

1. Technique of laryngeal ultrasound
2. Normal laryngeal anatomy on ultrasound
3. Ultrasound appearances of commonly encountered benign and malignant laryngeal pathology

Materials and methods :

We will use case material from our tertiary referral centre to demonstrate the main teaching points.

Results :

1. Technique for assessing the larynx with ultrasound
2. Normal laryngeal anatomy on ultrasound
3. Benign pathology - laryngocoeles, laryngeal mucocoeles, thyroglossal duct cysts and remnants including the rare malignant papillary carcinoma within a thyroglossal remnant
4. Malignant pathology - squamous cell carcinoma including evaluation of extent within the larynx and extralaryngeal spread to the tongue base, through the superior thyroid notch or cricothyroid region

Conclusion :

Laryngeal ultrasound is an under utilised but valuable skill for the head and neck radiologist. Ultrasound is complimentary to CT providing high resolution images in realtime, does not involve ionising radiation & can be used to guide FNA if require.

Ultrasound of the thyroid: a pictorial review

N.J. Stephens, S. Morley, A. Ahmed, T. Beale

University College London Hospital, London, UK

Poster Nr 40

Objective :

This pictorial review will demonstrate the ultrasound appearances of pathology of the thyroid gland.

Materials and methods :

We will be using examples from our tertiary referral centre to demonstrate the commonly encountered and rare pathologies.

Results :

We will describe how to assess the thyroid gland sonographically using grey scale, colour and power Doppler ultrasound techniques. We will describe the characteristic appearances of thyroid pathology with illustrative examples.

Congenital lesions

- Embryology
- Thyroglossal duct cyst remnants
- Ectopic thyroid

Inflammatory lesions

- Reidel's thyroiditis
- Hashimoto's thyroiditis

Benign focal lesions

- Colloid nodules
- Hyperplastic nodules

Neoplastic lesions

- Papillary carcinoma
- Medullary carcinoma
- Follicular carcinoma
- Anaplastic carcinoma
- Hurtle cell carcinoma
- Squamous cell carcinoma
- Lymphoma
- Metastases

All the pathologies depicted have been confirmed histologically.

Conclusion :

Our pictorial review describes the sonographic features of common and unusual pathologies affecting the thyroid gland.

Top ten tips for ultrasound guided FNA in the neck

N.J. Stephens, A. Ahmed, T. Beale, S. Morley

University College London Hospital, London, UK

Poster Nr 41

Objective :

A practical guide for performing FNA and core biopsy of masses in the neck using ultrasound guidance. To enable the reader to learn from our experience and optimise their practice.

Materials and methods :

We will use examples from our tertiary referral centre to demonstrate the main teaching points with text and illustrative examples.

Results :

Our experience of performing ultrasound guided FNA and core biopsy of neck lesions has enabled us to formulate top ten teaching points that we recommend for successful practice.

Conclusion :

Ultrasound guided FNA and core biopsy of lesions in the neck is a valuable tool. We have described the main pearls and pitfalls that we have encountered during our practice to enable to reader to improve their technique.

Does upper aerodigestive tract tumour site influence incidence of intrathoracic malignancy at initial staging?

D.B. Stobo, G.T.J O'Neill

Radiology Department, Glasgow Royal Infirmary, Glasgow, UK

Oral presentation

Objective :

To determine whether the relatively high incidence of intercurrent intrathoracic malignancy found at initial staging of upper aerodigestive tract tumours is dependent on the site of primary disease.

Materials and methods :

Retrospective review of reported findings at initial staging CT of neck and thorax for oral cavity, oropharyngeal, hypopharyngeal and laryngeal squamous cell carcinoma.

Results :

138 patients were identified in whom 10 (7.2%) had strong evidence of intrathoracic malignancy. None of the 36 patients with oral cavity disease had conclusive evidence of an intrapulmonary neoplasm. In contradistinction, 10 out of 102 patients with primary disease elsewhere had evidence of malignancy within the thorax. This difference in incidence reaches significance (Fisher's exact test $P < 0.05$). 24 (17%) had indeterminate findings, none of which were found to be significant at follow-up within the study period.

Conclusion :

A relatively high incidence of concurrent intrathoracic malignancy at staging of pharyngeal and laryngeal primary tumours is confirmed. The incidence appears lower in those primary tumours restricted to the oral cavity. These patients are unlikely to benefit from thoracic CT and, in most cases, should be offered single modality staging with MRI for superior local assessment. Indeed, screening of the thorax with CT in this subgroup may introduce unnecessary confusion and treatment delay given the high incidence of indeterminate scan findings requiring further investigation.

Squamous cell carcinoma perfusion at multi-detector row CT: reproducibility of tumor and muscle quantitative measurements, inter- and intra-observer agreement

K. Surlan-Popovic, Z. Rumboldt, T.J. Vogl, M.G. Mack, S. Bisdas

Department of Radiology, Johann Wolfgang Goethe University Hospital, Frankfurt, DE

Oral presentation

Objective :

To determine the reproducibility of squamous cell cancer (SCC) and muscle tissue perfusion measurements as well as the inter- and intra-observer agreement using dynamic contrast-enhanced multi-detector CT (MDCT).

Materials and methods :

Twelve patients with histologically proven SCC of the upper aerodigestive tract were examined using 16-MDCT. Perfusion studies were repeated within 46h. Measurement reproducibility as well as measurement error and repeatability were assessed for each of the four perfusion parameters using the Bland-Altman plots. Two independent observers recorded the perfusion values of the tumor tissue; inter- and intra-observer agreement was assessed using the Bland-Altman plot analysis and intraclass correlation coefficients.

Results :

For the tumor, the mean difference (95% limits of agreement) was 0.40 ml/min/100g tissue (?6.80, 9.60); 0.01 (?0.96, 0.97) mL/100g tissue; 0.20 (?1.80, 2.30) s; and 0.40 (?2.00, 2.80) ml/min/100g tissue for BF, BV, MTT, and PS, respectively. For the muscle, the mean difference (95% limits of agreement) was -0.18 (?1.70, 1.35), 0.04 (?1.17, 1.35), ?0.10 (?5.80, 5.60), and -0.10 (?2.20, 2.00), respectively. Measurement changes of at least $\pm 8\%$, 30%, 36%, and 13% were found to be significant for BF, BV, MTT, and PS, respectively. The intraclass correlation coefficients for inter-observer agreement ranged from 0.80-0.88. The intraclass correlation coefficients for intra-observer measurements ranged from 0.86-0.94.

Conclusion :

Quantitative perfusion measurements of SCC and muscle tissue are reproducible. Measurements from tumor are less variable than from skeletal muscle. There is better intra- than inter-observer agreement.

Perfusion CT of the cervical spinal cord: feasibility and reproducibility of the method and interchangeability of the perfusion estimates between two software packages

K. Surlan-Popovic, Z. Rumboldt, M.V Spampinato, T.J. Vogl, M.G. Mack, S. Blsdas

Department of Radiology, Johann Wolfgang Goethe University Hospital, Frankfurt, DE

Poster Nr 42

Objective :

To examine the feasibility of perfusion CT studies of the cervical spinal cord, to examine the reproducibility of the technique, the interchangeability of the values obtained by two different commercially available post-processing software packages.

Materials and methods :

The perfusion CT studies of 40 patients with tumors in the head and neck were retrospectively identified and post-processed using two different software packages (Software 1: deconvolution-based analysis with adiabatic tissue homogeneity approach and Software 2: maximum-slope-model with Patlak analysis). Eight patients were examined twice after a median of 46 h (36-68) in order to assess the reproducibility of the perfusion measurements. Two neuroradiologists separately generated two sets of calculation for each patient, corresponding to two selections of the arterial input function (AIF) for comparison: (i) the larger of the two internal carotid arteries (ICA) and (ii) the vertebral artery (VA). Perfusion maps that represented blood flow (F) in mL/min/100g, blood volume (V) in mL/100 g, mean transit time (MTT) in seconds (s), time to peak (tp) (in s), and permeability (PS) in mL/min/100g were generated. Parametric and non-parametric tests for comparison between subjects in the same sa

Results :

The medians of F, V, MTT, PS, and tp parameters obtained with the Software 1 with AIF in the ICA as well as AIF in the VA were 6.02, 1.00, 14.72, 1.03, 4.5 and 6.87, 1.11, 15.41, 0.9, 5 respectively. V and MTT values revealed statistically significant differences between the two AIFs (p-value \leq 0.03). With the Software 2 the F and V values were different between the two AIFs (p-value=0.02). The ? coefficients were 0.95-1.00. The BA plots showed satisfactory limits of agreement. Only PS using Software 1 showed a within-subject coefficient of variation >50%. The significant changes for a single patient (%) using Software 1 were \pm 120%, 90%, 180%, and 250% for F, V, MTT, and PS, respectively. Significant changes for a single patient (%) using Software 2 were \pm 110%, 80%, and 130% for F, V, and PS, respectively. The degree of agreement between the two software packages was acceptable only for F and PS values.

Conclusion :

Perfusion CT of the cervical spinal cord is feasible. The reproducibility of the techniques is satisfactory. The perfusion values are dependent on the AIF site. There is interchangeability of the results only for F and PS values.

Evaluation with cranial computed tomography as a prognostic factor for head injuries in children and young adolescents

N. Syrmos, G. Gavridakis, E. Astropekaki, K. Grigoriou, V. Valadakis, D. Arvanitakis, L. Triantafyllou

Venizeleio General Hospital, Neurosurgical and CT-scan Department, Heraklion and Thessaloniki, GR

Poster Nr 43

Objective :

Aim of our study was to determine clinical characteristics and outcome of head-injured children and young adolescents admitted to the emergency department of a second level hospital and to evaluate the use of neuroimaging as a prognostic factor of morbimortality in these patients.

Materials and methods :

We performed a 10-year retrospective review (1998-2008). We included all patients with severe head injury admitted to our hospital. Clinical summaries and imaging studies were reviewed. Data for 199 patients, aged 1 to 22 years, were collected.

Results :

We reclassified neuroimaging patterns into 2 groups: FIRST GROUP- those with few imaging findings ?SECOND GROUP- those with important lesions. The 2 subgroups were retrospectively reviewed for 1.mechanism,2. age, 3.Injury Severity Score, 3.GCS score,4. associated injuries, and 5.CT scan findings (normal, fracture only, or intracranial injury). We classified patients intoA- favorable evolution,B- moderate disability, and C-unfavorable evolution. Poorer evolution correlated with poorer initial neuroimaging patterns

Conclusion:

1. A normal neurologic exam and maintenance of consciousness does not preclude significant rates of intracranial injury in children and young adolescents trauma patients.
2. Skull fractures and superficial craniofacial injury are similarly unreliable. Identification of these patients is important for the occasional case requiring intervention and for the tracking of complications.
3. CT scanning is warranted for children and young adolescents patients with a high-risk mechanism of injury despite maintenance of normal neurologic status.

Traumatic brain injuries in rural areas of Crete

N. Syrmos, G. Gavridakis, E. Astropekaki, K. Grigoriou, V. Valadakis,
D. Arvanitakis, L. Triantafyllou

Venizeleio General Hospital, Neurosurgical and CT-scan
Department, Heraklion and Thessaloniki, GR

Poster Nr 44

Objective :

The aim of our study was to describe epidemiological and medical aspects of 100 cases of traumatic brain injury (TBI) from rural areas of Crete with total population of 800,000 inhabitants.

Materials and methods :

Median age was 41 years, range 1-99 years; 70% were men and 30% were women; 5% children 0-14 years, 45% adults 15-64 years, and 50% elderly persons 65-91 years old. Severity classification was based on Glasgow Coma Scale (GCS) on arrival-26 mild TBI 97% (GCS 13-15), moderate 1% (GCS 9-12), and severe 2% (GCS 3-8).

Results :

The most common injury events were falls (55%) and vehicle-related events (30%). The percentage of falls was high among elderly persons but among adults vehicle-related injury events were also prominent. At least 20% of all patients were under the influence of alcohol, especially adult male bicyclists.

Conclusion :

CT was performed on 66 cases (66%) revealing 26 cases with intracranial hemorrhage (ICH) which is 39.3 % of the examined or 26 % of all the injured. The rate of ICH increased with increasing age and also increased with decreasing GCS . Attention should be directed to acute management of mild TBI in order to detect potentially dangerous ICH as well as to preventive actions against falls and vehicle related accidents.

The accuracy of 3D CBCT in diagnosis and treatment planning of dentofacial deformities

L. Trevisiol, E. Grendene, A. D'Agostino, G. Bissolotti, G. Corrocher, R. Maroldi, M. Pregarz, P.F. Nocini

Verona, IT

Poster Nr 45

Objective :

The aim of this study is to understand if measurements obtained by Cone Beam Computed Tomography (CBCT) are more specific and consistent than those obtained by a traditional ceph.

Materials and methods :

23 skeletal landmarks were located on a dry skull and 20 measurements were calculated directly on the skull by means of a digital calibrate caliper. A traditional ceph of the skull was acquired using the Sirona-Orthophos Plus DS/ Plus DS Ceph while the volumetric data with the QR Newtom 3G CBCT. The CBCT volume was imported in a specifically designed software (Dolphin 3D, Dolphin Software), in order to create a 3D model of the skull, mark the landmarks directly on it and then generate from it a 2D ceph with the same perspective distortion ratio as a traditional one and a 2D ceph with orthogonal projection (ratio 1:1). A further 3D digital model was created by a Newtom software (NNT). Once obtained these new images the 20 measurements were calculated both on the 3D models (Dolphin ? NNT), on the generated 2D cephs and on the traditional ceph. All the obtained measurements (skull, traditional ceph, 3D CBCT, 2D generated ceph) were statistically compared.

Results :

In order to evaluate the accuracy of a 3D imaging system based on CBCT a comparative study has been projected between this system and a traditional 2D cephalometric one. All the data showed that measurements from CBCT synthesized cephalograms are similar to those based on conventional radiographic images with no statistically significant discrepancies, both if the measures are calculated on perspective and orthogonal cephs. Also 3D models measurements showed an high level of accuracy compared to the skull. Suitable softwares in elaboration of CBCT volume are of paramount importance to obtain accurate and informative data. Cone Beam Computed Tomography (CBCT) represents a main change in maxillo-facial digital imaging both for diagnosis and treatment planning. This kind of device presents many advantages as low dose radiation, no distortion of image and large field of investigation.

Conclusion :

3D CBCT models could open a new frontier in the field of surgical deformities diagnosis and treatment planning restating the goals of cephalometry, however further studies will be necessary to develop reliable referring database and standard analyses.

CT perfusion examination is useless in evaluation of mandibular infiltration by malignant tumor - true or false ?

A. Trojanowska, P. Trojanowski, W Olszanski, J Klatka, A. Drop

University Medical School of Lublin, Department of Radiology, Lublin, PL

Oral presentation

Objective :

To evaluate if computed tomography perfusion (CTP) examination might be used as a valuable tool in determination of mandibular infiltration by a malignant tumor.

Materials and methods :

during last 20 months 18 patients with oral cavity squamous cell carcinoma (SCC) adjacent to the mandible were examined. In all patients standard contrast-enhanced computed tomography examination (CECT) of head and neck region was performed (100 ml of iodinated, non-ionic contrast medium, flow 1 ml/s, delay 100 s) in 1.25 mm slices, reconstruction kernels ? bone plus and soft tissue. Immediately afterwards CTP examination was performed at the level of tumor (8 cm coverage), in 2.5 mm slices. Basic parameters for perfusion were obtained (rBF, rBV, MTT, PS) and perfusion maps were automatically created based on CT Perfusion 4 software (GE Healthcare, Milwaukee, USA). All patients underwent surgery ca 10 days after imaging, with fragmental, marginal, or no mandible removal. The extent of removal was decided based on standard CECT studies and intra-operative findings. Surgical specimens underwent histological analysis and results were compared with CTP findings.

Results :

In the group of 18 examined patients, 9 underwent mandibular removal (6 fragmental and 3 marginal). In 8 cases infiltration was confirmed on histology. In this group, only in 2 cases CTP findings were suggestive of mandibular invasion (elevated values of rBF, rBV and PS) . Based on CECT studies in bone and soft tissue window it was possible to determine mandibular invasion in 5 cases (3 cases of medullary invasion and 2 cases of cortical invasion), which was also confirmed on histology.

Conclusion :

Study shows no evidence that CTP examination may be a useful adjunct in determination of possible mandibular infiltration by SCC. Conventional CECT study with bone kernel reconstructions show better results in defining cortical and medullary invasion.

MRI findings in the neck of survivors of strangulation

D.W. Tshering, H.C. Thoeny, S. Ross, D. Spendlove, S. Bolliger, M.J. Thali, P. Vock, L. Oesterhelweg, A. Christe

Department of Diagnostic, Interventional and Pediatric Radiology and Department of Forensic Medicine, Inselspital, University of Bern, Bern, CH

Oral presentation

Objective :

To assess the pattern of injury in the head and neck area in survivors of strangulation.

Materials and methods :

A consecutive series of 57 patients (17 male, 40 female) with a median age of 27 years, range 12-50 years, underwent MRI of the head and neck within a mean time of 11 hours (range 2-55hours) after strangulation. The study was performed on a 1.5T MR unit with axial T1-weighted sequences with and without fat saturation, axial T2-, TIRM and TrueFisp-sequences with a slice thickness of 4mm and an intersection gap of 1mm. Two radiologists analysed the images for soft tissue changes, laryngeal, salivary glands and thyroid involvement as well as vessel injury and lymph node alterations.

Results :

Intracutaneous signal alteration was found in 28% (16/57), subcutaneous changes in 58% (33/57) and intramuscular alteration in 25%(14/57), thickening of the platysma was found in 30% (17/57), edema of the glottis was observed in 9% (5/57), perilaryngeal bleeding or edema in 14% (8/57), cartilage and hyoid fractures not seen, peripharyngeal alterations in 12%(7/57), submandibular alteration in 7% (4/57), parotid hemorrhage or edema in 7% (4/57), Thyroid gland alteration in 4% (2/57). No vessel rupture or intramural hematoma or dissection was seen. Edema or haemorrhage of the lymphnodes were observed in 23% (13/57) and lymphnodes were enlarged in 30% (17/57). There were no changes in 16% of patients (9/57). Enlargement of lymph nodes is a non-specific finding and if these are excluded, 37% (21/57) were normal.

Conclusion :

MRI allows detection of subtle changes in different neck regions after strangulation and might therefore be a helpful noninvasive tool in forensic medicine helping to better judge the severity of strangulation.

The role of DW-MRI in the differentiation of tumor and posttherapeutic changes after radiotherapy of laryngeal or hypopharyngeal cancers

D.W. Tshering, S. Simon-Zoula, P. Zbaeren, A. Geretschlaeger, H.C. Thoeny

Department of Diagnostic, Interventional and Pediatric Radiology, Department of Oto-Rhino-Laryngology, Head and Neck Surgery, and Department of Radiation Oncology, Inselspital, University of Bern, Bern, CH

Oral presentation

Objective :

The aim of this study was to evaluate the accuracy of Diffusion-weighted MRI (DW-MRI) as a non-invasive technique to differentiate between posttherapeutic changes and recurrent/residual tumor after radiotherapy of a laryngeal or hypopharynx

Materials and methods :

Twelve patients (10 male, 2 female, median age: 58, age range: 49 ? 74 y) with newly developed symptoms after radiation therapy of the neck for tumors of the larynx (n=11) and hypopharynx (n=1) were imaged on a 1.5T MR unit (SONATA, Siemens, Germany). We performed conventional axial T1 and T2 weighted images as well as coronal inversion recovery sequences before contrast injection, followed by DW-MRI in the axial plane with 6 diffusion gradient b-values (0, 50, 100, 500, 750 and 1000 sec/mm²) with the same geometry as the conventional sequences (slice thickness=3mm, intersection gap=1mm and 3 averages with a TR of 7100 and a TE of 75msec). Finally axial and sagittal T1 weighted imaging with fat saturation was performed after intravenous Gadolinium injection. Two experienced radiologists performed visual analysis of the b=1000 images and the ADC map. Hyperintense signal on b=1000 images corresponding to hypointense signal on the respective ADC map was interpreted as tumor tissue where

Results :

Of the twelve patients, six had tumor recurrence and six patients did not have tumor as proven on histology. ADC values were lower for patients with tumor with a mean value of 104 (range 79-118mm²/s) as compared to those without tumor with a mean value of 178 (range 127-207 mm²/s). DW-MRI was able to correctly diagnose 5 out of 6 patients with tumor recurrence and correctly identify all patients without tumor recurrence. One patient with tumor was classified as indeterminate visually and falsely negative according to the diffusion values.

Conclusion :

The present study suggests that DW-MRI is a very promising non-invasive tool in differentiating between tumor tissue and post therapeutic changes in patients with laryngeal and hypopharyngeal tumors treated with radiotherapy and surgery.

Maxillary sinus findings in relation to dental findings

J. Vallo, L. Suominen-Taipale, A. Norblad, S. Huuonen, K. Soikkonen

Department of Oral Radiology, Institute of Dentistry, University of Helsinki and National Public Health Institute (KLT), Department of Health and Functional Capacity, Helsinki, FI, Institute of Clinical Dentistry, University of Tromso, Tromso, NO

Poster Nr 46

Objective :

The aim of this study was to define the prevalence of radiographically assessed maxillary sinus findings and to establish the extent to which the findings are related to pathologic dental findings in a nationally representative sample.

Materials and methods :

Study sample consisted of 5 021 participants 30 years or older of a nationally representative Health 2000 Health Examination Survey examined by means of panoramic radiography (2 812 women and 2 209 men). The mean age was 51.7 years. Panoramic radiographs were taken with a digital PM 2002 radiographic apparatus (Planmeca 2002 CC Proline, Planmeca Oy, Helsinki, Finland). Outcome of the present study were findings in the maxillary sinus that were recorded and categorized into three groups: mucous thickening, mucosal antral cyst (MAC) or some other finding. Any pathologic finding in the maxillary sinus was also recorded. Periapical lesion, horizontal alveolar bone loss, vertical infra bony pockets, furcation lesions and root canal treatments were recorded. For the analyses, age was grouped into five categories: 30-39 years old, 40-49 years old, 50-59 years old, 60-69 years old and 70 years or older. Analyses were also performed separately in right and left premolar and molar area.

Results :

Mucosal changes in the maxillary sinus were found in 19% of the subjects. Findings were more common in men (27%) than in women (13%), p

Conclusion :

In conclusion this nationally representative study dental pathologic findings should be taken account as an etiologic factor for mucous thickening but not for MACs.

Diagnostic yield of MRI for audiovestibular dysfunction using contemporary referral criteria: correlation with presenting symptoms and impact on clinical management

C. Vandervelde, S. Connor

Guy's and St Thomas' NHS Foundation Trust, London, UK.

Oral presentation

Objective :

To investigate the diagnostic yield of T2 weighted MRI for vestibular schwannoma and other relevant pathologies in the setting of audiovestibular symptoms and contemporary more liberal referral criteria.

Materials and methods :

881 consecutive MRI scans performed in patients with audiovestibular symptoms were reviewed. Clinical indications and scan findings were recorded. Case notes were reviewed in patients with positive imaging findings. Two-way cross-tabulation Chi-square analysis was performed to assess the relationship between presenting symptoms and imaging outcome.

Results :

12/881(1.4%) were positive for vestibular schwannoma. A further 4/881(0.4%) revealed other relevant pathology. Incidental pathologies, felt to be irrelevant to the presenting symptoms, were noted in 12/881(1.4%). In all 12 cases which were positive for vestibular schwannoma, either tinnitus or hearing loss was present. No clinical presentation seemed to be able to predict a positive or negative imaging outcome with statistical significance reflecting the overall diagnostic yield in the population of patients imaged.

Conclusion :

The yield for T2 weighted MRI to diagnose vestibular schwannoma is lower than previous studies, likely to reflect trends in referral criteria. No single symptom or combination of symptoms is a statistically significant predictor of imaging outcome.

Brachial plexus and tractography (DTI)

M.I. Vargas, M. Viallon, R. Kohler, M. Becker, K.O. Lövblad, S. Altrichter, J. Delavelle

Department of Radiology, Division of Neuroradiology Geneva University Hospital, Geneva, CH

Poster Nr 47

Objective :

The aim of this study was to assess the clinical utility of DTI in patients with diseases of the brachial plexus.

Materials and methods :

Imaging was performed on a total of 28 examinations: 21 patients (eleven men and ten women, aged between 17 and 81 years) and 6 volunteers. All patients with a suspicion of clinical lesions of the brachial plexus have been examined with a 1.5 AVANTO system with T2 and T1 weighted images, STIR3D and DTI images with the gradients in 30 orthogonal directions. Maps of the apparent diffusion coefficient and of fractional anisotropy were reconstructed. All tumours have been biopsy proven.

Results :

Three patients had primary neurogenic benign tumors, six patients had secondary tumors, one had lymphoma with perineural dissemination, one patient had primary pleural tumor, three patients had osteoarthritis, one had traction bronchiectasis (antecedent tuberculosis), one had meningocele, one had thoracic outlet syndrome and four patients were normal. We demonstrate here that DTI with fiber tracking reconstruction can demonstrate nerves tracts and their alterations or deformation due to pathological processes located surrounding or along the brachial plexus. The DTI show deformation, infiltration or destruction the trunks or cords of the brachial plexus. The technique appears very important for surgical and oncologic planning.

Conclusion :

We think that the diffusion tensor and tractography offers a novel approach to image to brachial plexus for detection, analysis and surgical planning the lesions.

Intraoperational control of dental implantation with digital microfocal radiography

A.Y. Vasiliev, N.S. Serova, A.I. Ushakov

Moscow State University of Medicine and Dentistry, Moscow, RU

Poster Nr 48

Objective :

Evaluation of microfocal radiography possibilities at the intraoperational stage of stomatological implantation.

Materials and methods :

25 patients were examined (10 female and 15 male) with an age from 19 to 56. Mandibular implantation was performed to 17 patients, maxillary ? 8 patients. The examination was performed inside the operation room with portable digital microfocal radiography unit with the following exposition parameters: 60 kV, 0.1 mA, exposition time ? 0.2 s.

Results :

Data obtained had allowed correct relationship of implantation space and surrounding anatomical structures during the operation. 12 mandibular patients had indicated impermissible distance from the lower wall of implantation space to the mandibular canal (less than 1.8 mm) and in 3 patients distance to foramen mental was less than 1.4mm. Maxillary bone tissue volume among the examined group was sufficient for implant installation. Intraoperational microradiography had allowed surgeon to make decision on implantation technique which differed from preplanned one based on preoperative radiology examinations (orthopantomography and spiral CT): in 8 cases decision was done to decrease the depth of implant installation and in 4 cases ? installing the implant with a smaller size, compared to preplanned.

Conclusion :

Use of portable microfocal radiography units in the intraoperative stage of stomatological implantation allows to make final decision during the operation itself about the tactic of performing. This significantly increases the quality of treatment.

Difficulties in differential diagnosis of head and neck cystous formations

M.V. Vykluk, A.Y. Vasiliev, I.N. Gipp

Moscow State University of Medicine and Dentistry, Moscow, RU

Poster Nr 49

Objective :

Materials and methods :

Ultrasound examination was performed at 268 patients with an age from 2 to 56, with cystous formations of head and neck area.

Results :

Branchial cysts were found at 62 patients: in 34 cases typical sonographic signs were present. At the inflammation period difficulties had appeared when cyst looked like an avascular formation with indistinct irregular contour and heterogeneous content. In 5 cases medial neck cysts demonstrated atypical form, thick capsula and heterogeneous content, but multiple station study showed connections between chambers and hyoid bone. The determination of large size cysts was difficult at submandibular localization. But mouth floor examination had always demonstrated the connection between the cyst and sublingual salivary gland. Dermoid cysts were visualized as cavitory formations with multiple echogenic inclusions. Inflammation complication had made lymphangioma differential diagnostics difficult. Structure of cystous lymphangiomas was characterized by liquor cavities of prolate form with singular or multiple septums. Cavernous component was determined as small size hypo-echogenic zones.

Conclusion :

High resolution sonography allows to determine the nosology and the extent of the pathology. This has a positive influence upon the optimal treatment tactics choice.

MRI of parotid tumors: typical lesion characteristics in MR improve discrimination between benign and malignant disease

C. Waldherr, A. Christe, P. Zbären, E. Stauffer, H.C. Thoeny

Department of Diagnostic, Interventional and Pediatric Radiology, Inselspital, University of Bern, Bern, CH

Oral presentation

Objective :

To determine whether malignant and benign parotid lesions can be discriminated by MR imaging.

Materials and methods :

Ninety consecutive patients (m: 46, f: 44; median age: 57y; range: 15-86y) with parotid gland tumours who underwent MRI before undergoing surgery were retrospectively analyzed. Axial T1-, T2-weighted and TIRM sequences and axial, coronal and sagittal contrast-enhanced fat-suppressed T1-weighted images were acquired with a 1.5-T MR unit. Histology was available of all tumours. Following MR parameters were analyzed: signal intensity (in the respective sequence), margins (well vs. ill-defined margin), localization (deep/superficial lobe), extension into neighbouring structures, growth patterns (circumscribed, diffuse), perineural spread, and contrast enhancement (marked/poor; homogeneity).

Results :

Histology revealed 54 benign lesions (adenoma: n=32; Warthin tumor: n=16, epidermoid cyst: n=2; oncocytoma: n=3; papilloma: n=1), and 36 malignant (adenoid cystic carcinoma (ca): n=8; lymphoma: n=2, mucoepidermoid ca: n=6, salivary duct ca: n=2, squamous-cell-ca-metastases: n=10, malignant myoepithelioma: n=1, acinic cell ca: n=3, malignant lymphoepithelial tumor: n=1, sarcoma: n=2, undifferentiated ca: n=1). Substantial discriminative factors for malignancy were: T2 intermediate signal intensity (p=0.008), blurred margins pre- contrast (p=0.001), and post-contrast (p=0.06), deep lobe localization (p=0.06), extension into both lobes (p=0.0003), diffuse growth pattern (p=0), perineural spread (p=0), and infiltration of neighbouring structures (p=0). Contrast enhancement is not a discriminative factor (p=0.7).

Conclusion :

A combination of different MR parameters (T2 intermediate signal intensity, blurred pre- and post-contrast margins, extension into both lobes, diffuse growth pattern, perineural spread, and infiltration into neighbouring structures) is highly suggestive for malignancy.